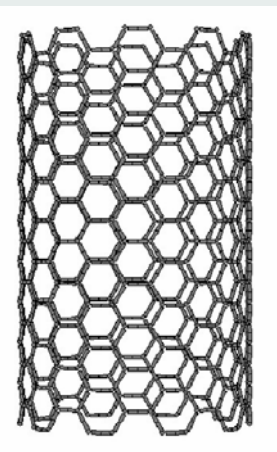
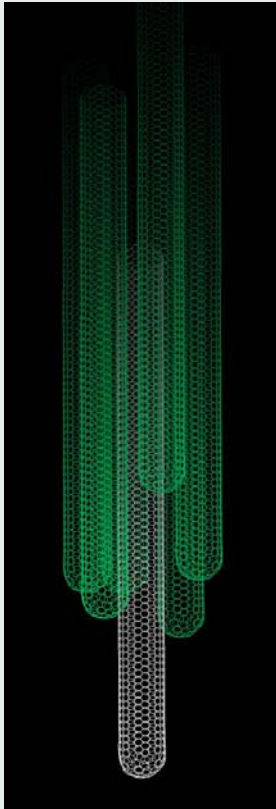


Carbon Nanotubes - CNTs

R. NESPER ETH ZÜRICH & COLLEGIUM HELVETICUM



06.11.2006

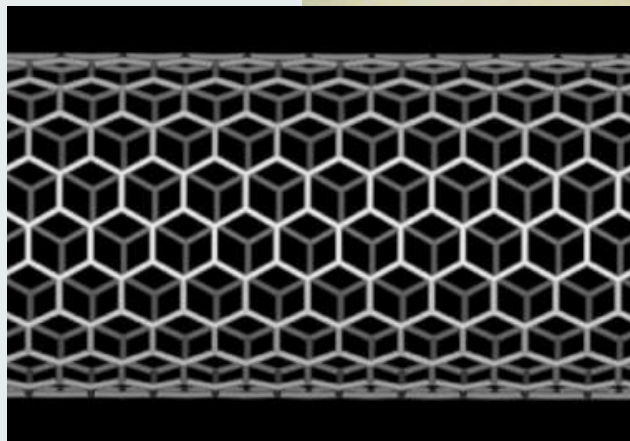
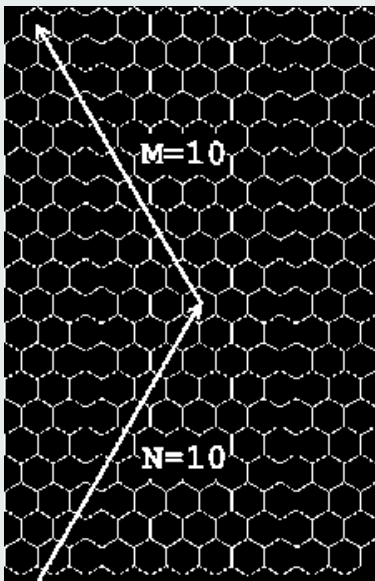
R. Nesper Oslo Lectures
Nanochemistry UIO

1



SWCNTs - Single Wall Carbon Nanotubes

R. NESPER ETH ZÜRICH & COLLEGIUM HELVETICUM



06.11.2006

Nanochemistry UIO

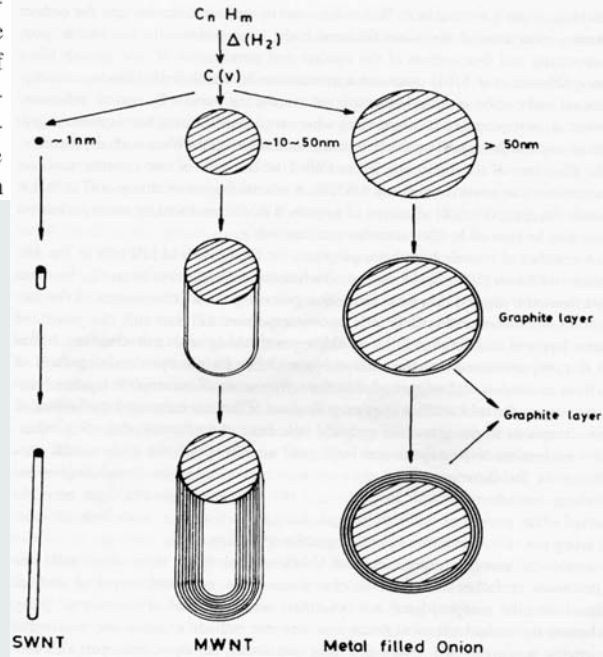
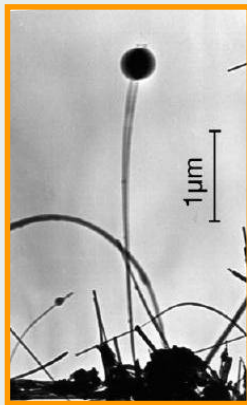
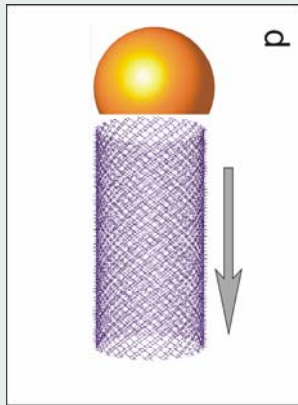
2



Carbon Nanotubes - Growth

good physical and chemical properties.^[1-3] Various methods for the synthesis of CNTs have been reported: arc-discharge,^[3,4] laser ablation,^[5] chemical vapor deposition,^[6-10] flame synthesis,^[11] and Smalley's recent invention of the high-pressure carbon monoxide (HIPCO) process.^[12] However, none of these methods can be used at low temperature, so the synthesis of CNTs with low-melting point materials, such as organic polymers, has been severely limited. Furthermore, expensive vacuum equipment is necessary to lower the temperature of the synthesis.^[13-16] Therefore, the strategy frequently used has been

R. NESPER ETH ZÜRICH & COLLEGIUM HELVETICUM



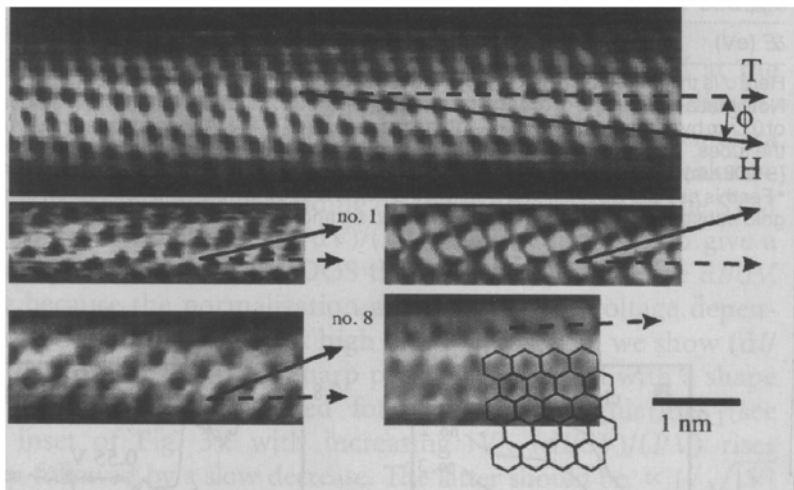
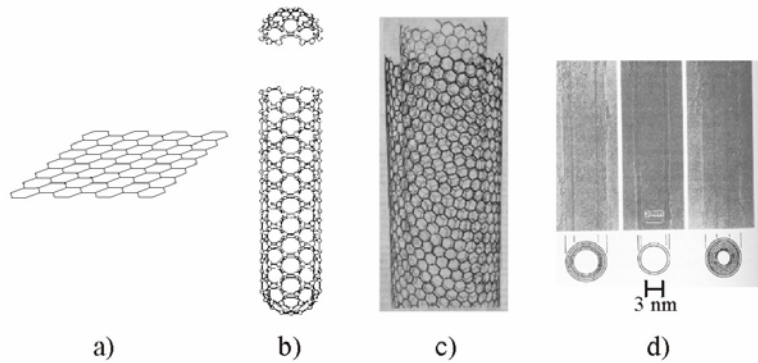
06.11.2006

R. Nesper Oslo Lectures
Nanochemistry UIO

3

Carbon Nanotubes - Building Principles

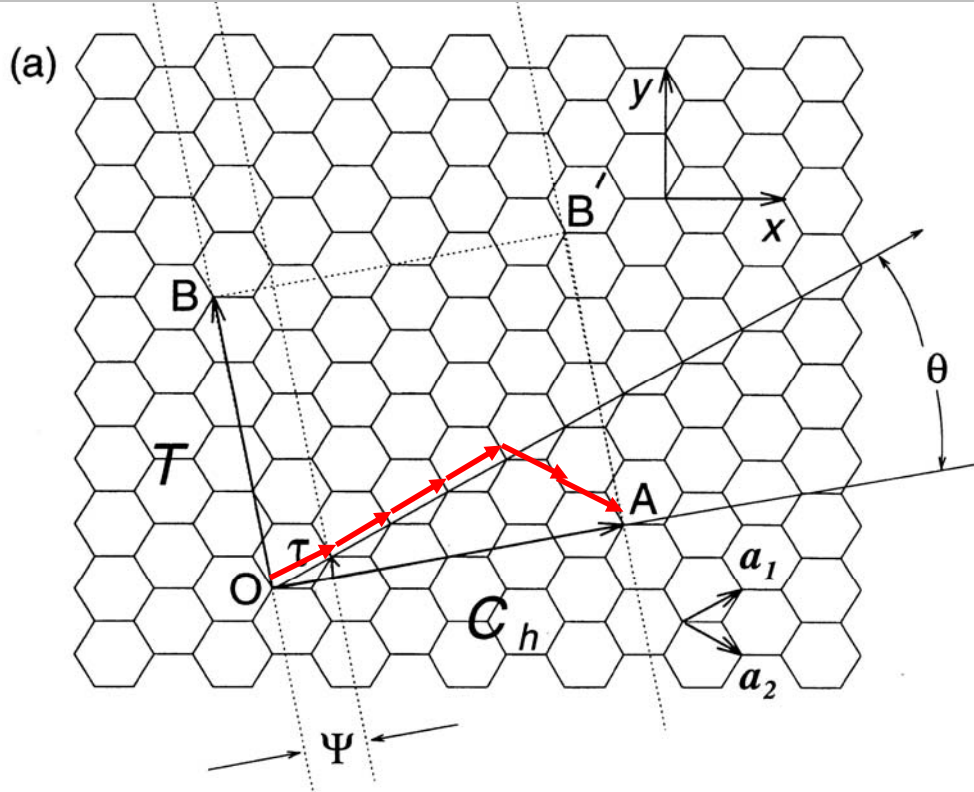
R. NESPER ETH ZÜRICH & COLLEGIUM HELVETICUM



06.11.2006

ETH
Empfohlen von: Technische Hochschule Zürich
Schweizerischer Nationalrat der Wissenschaften und
Technischen Universität München

Carbon Nanotubes - Building Principle



06.1

Carbon Nanotubes - Building Principle

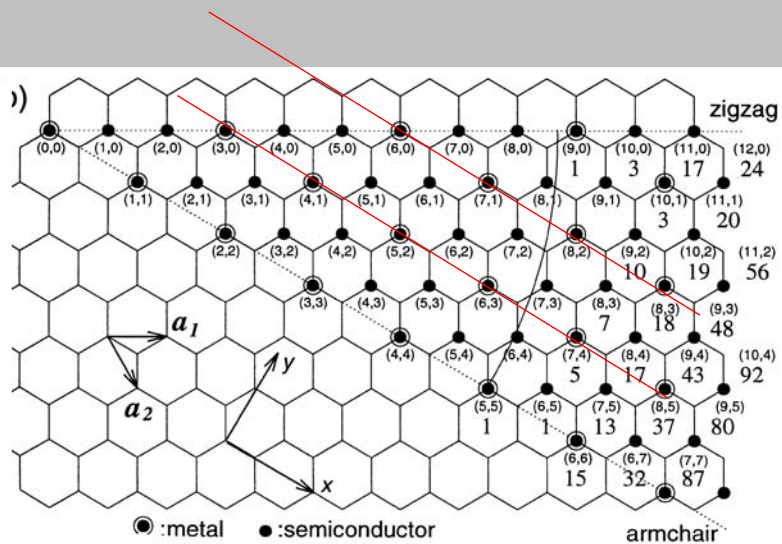


Fig. 19.2. (a) The chiral vector \vec{OA} or $C_h = na_1 + ma_2$ is defined on the honeycomb lattice of carbon atoms by unit vectors a_1 and a_2 and the chiral angle θ with respect to zigzag axis. Along the zigzag axis, $\theta = 0^\circ$. Also shown are the lattice vector $OB = T$ of the unit cell and the rotation angle ψ and the translation τ which constitute the symmetry operation $R = (\psi|\tau)$ for the carbon nanotube. The diagram is constructed for $(n, m) = (4, 2)$. (b) Possible vectors specified by the pairs of integers (n, m) for general carbon nanotubes, including zigzag, armchair, and chiral tubules. Below each pair of integers (n, m) is the number of distinct caps that can be joined continuously to the carbon tubule denoted $N(n, m)$ [19.4], as discussed in §19.2.3. The encircled dots denote metallic tubules while the solid dots are for semiconducting tubules.

06.11.2006

Carbon Nanotubes - Building Principles

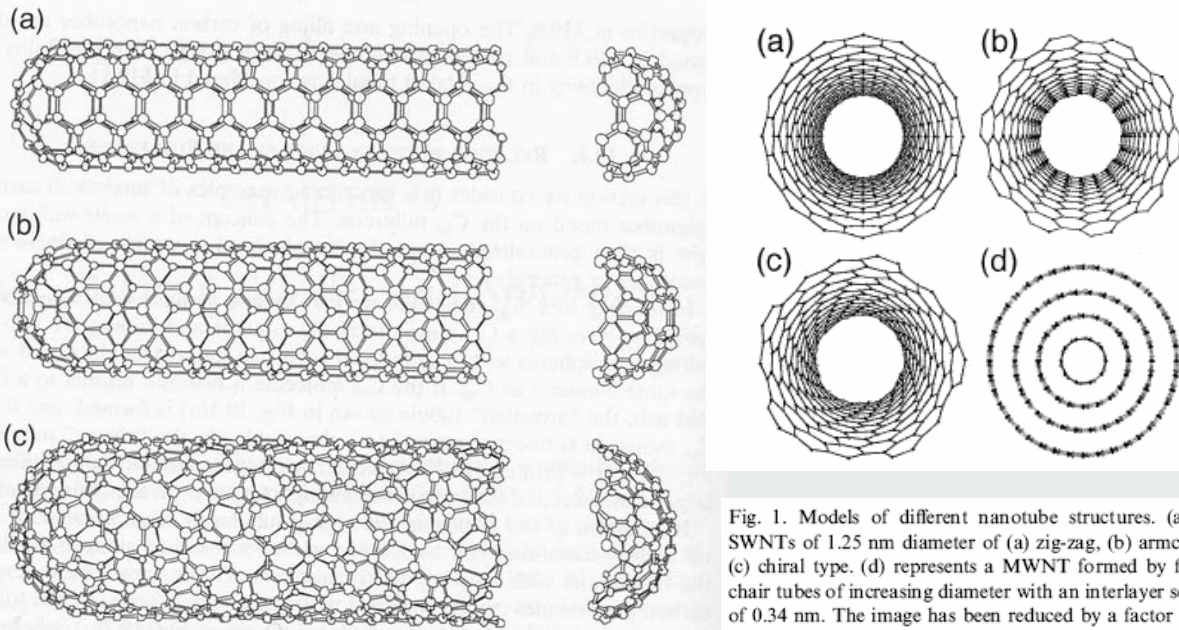
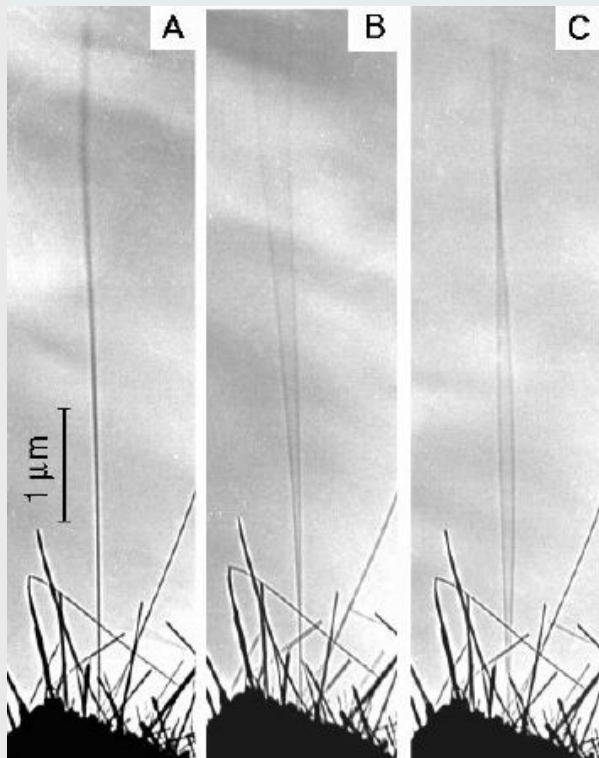


Fig. 19.1. By rolling a graphene sheet (a single layer from a 3D graphite crystal) into a cylinder and capping each end of the cylinder with half of a fullerene molecule, a “fullerene-derived tubule,” one atomic layer in thickness, is formed. Shown here is a schematic theoretical model for a single-wall carbon tubule with the tubule axis normal to: (a) the $\theta = 30^\circ$ direction (an “armchair” tubule), (b) the $\theta = 0^\circ$ direction (a “zigzag” tubule), and (c) a general direction $0 < \theta < 30^\circ$ (see Fig. 19.2) (a “chiral” tubule). The actual tubules shown in the figure correspond to (n, m) values of: (a) (5, 5), (b) (9, 0), and (c) (10, 5) [19.5].

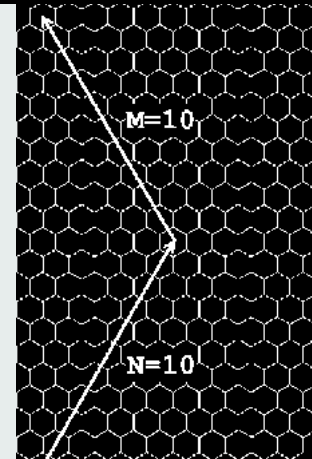
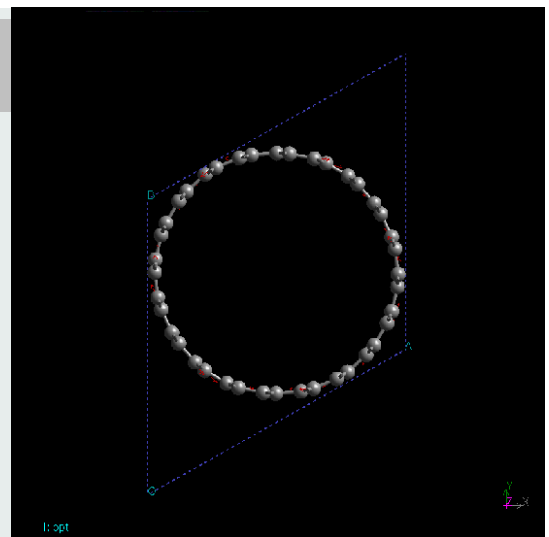
Fig. 1. Models of different nanotube structures. (a)–(c) are SWNTs of 1.25 nm diameter of (a) zig-zag, (b) armchair, and (c) chiral type. (d) represents a MWNT formed by four armchair tubes of increasing diameter with an interlayer separation of 0.34 nm. The image has been reduced by a factor of 2 with respect to images (a)–(c). The images have been generated with the software Mathematica 4.0 using a notebook by Brandbyge [197] that allows one to draw the structure as well as to compute the energy bands of SWNTs.

Dynamics of C-NTs

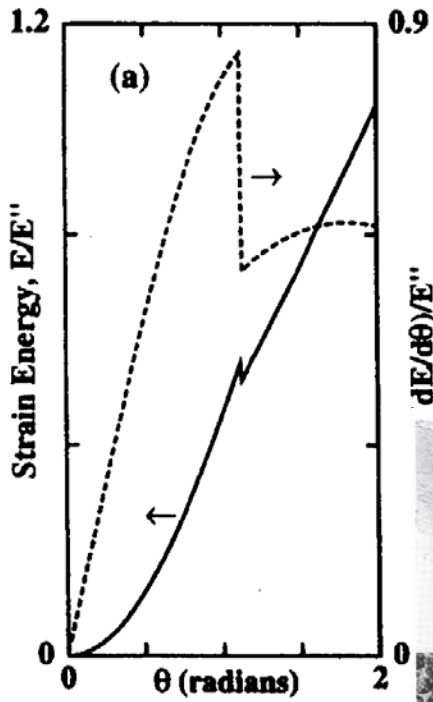


06.11.2006

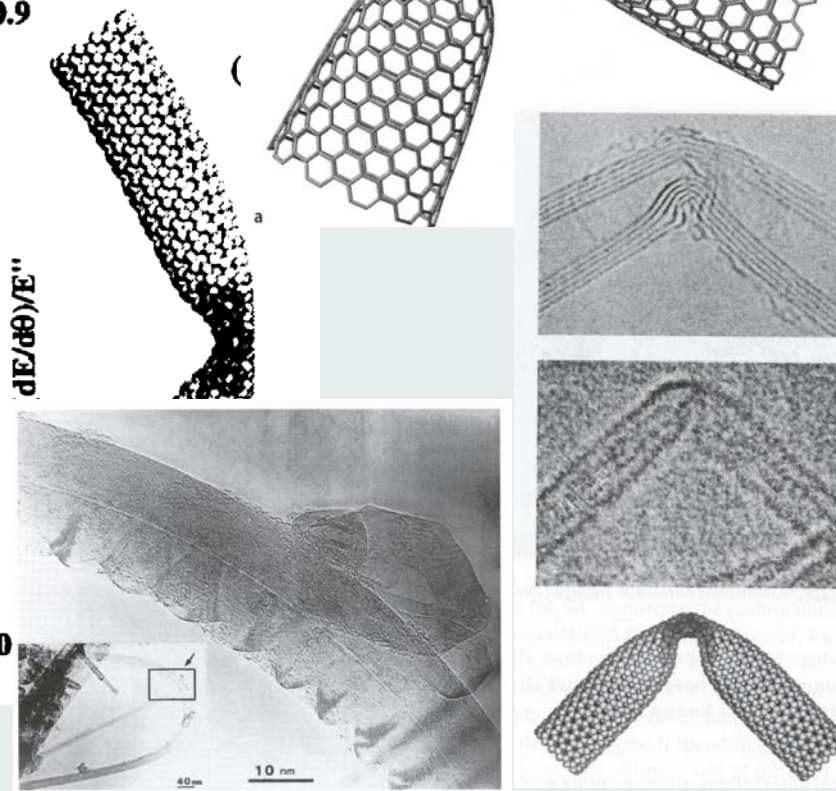
R. Nesper Oslo Lectures
 Nanochemistry UIO



Strength of CNTs

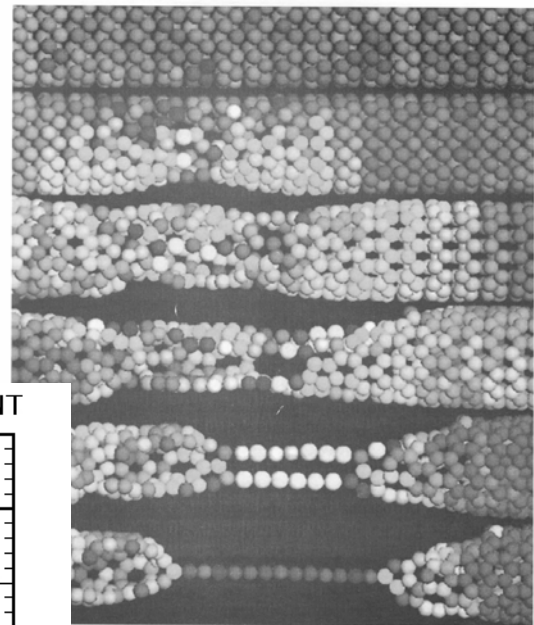


06.11.2006

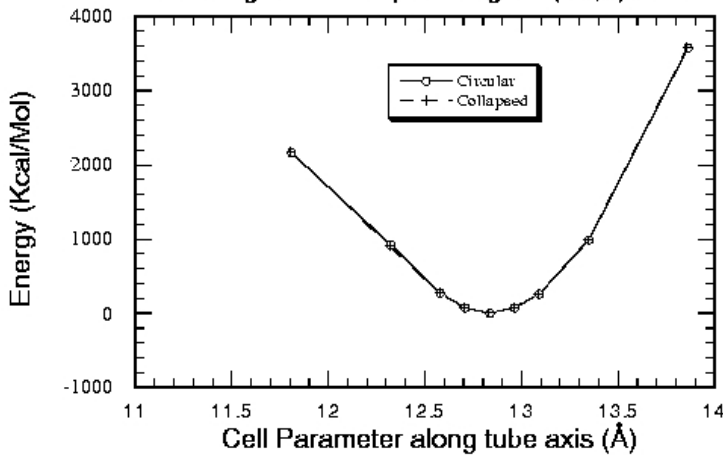


Strength of CNTs

SIUM HELVETICUM



Stretching and Compressing of (80,0) SWNT



06.11.2006

SWCNT - Plastic Deformation

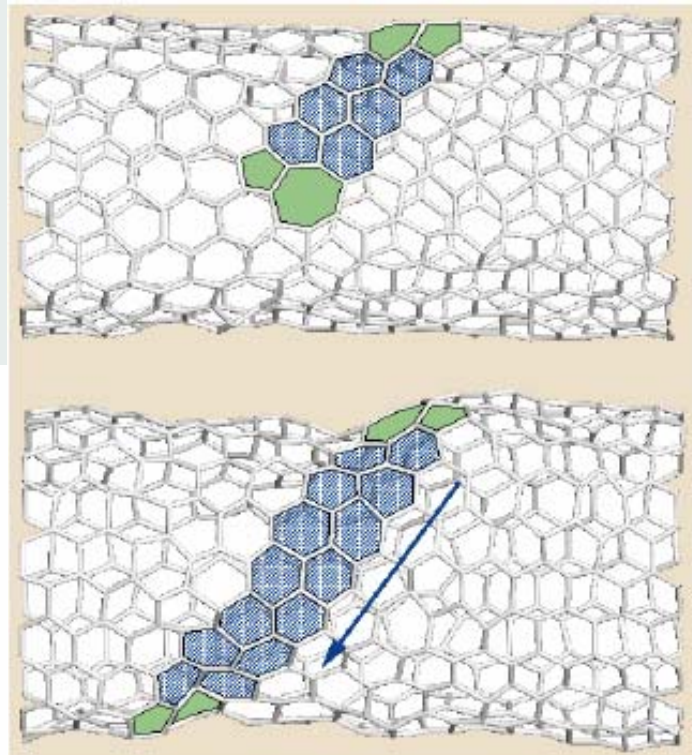


Figure 1 Plastic deformation of a carbon nanotube. Molecular dynamics simulations of a (10,10) nanotube under axial tension (J. Bernholc, M. Buongiorno Nardelli and B. Yakobson). Plastic flow behaviour is shown after 2.5 ns at $T = 3,000$ K and 3% strain. The blue area indicates the migration path (in the direction of the arrow) of the edge dislocation (green). This sort of behaviour might help make composite materials that are really tough (as measured by their ability to absorb energy).

06.11.2006

R. Nesper Oslo Lectures
 Nanochemistry UIO

11

Carbon Nanotubes

<http://www.pa.msu.edu/cmp/csc/nanotube.hmt/>

Characterization of each individual set of nanoparticles necessary

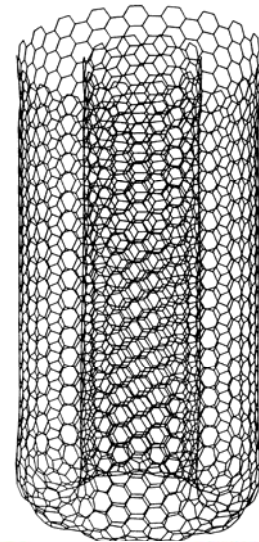
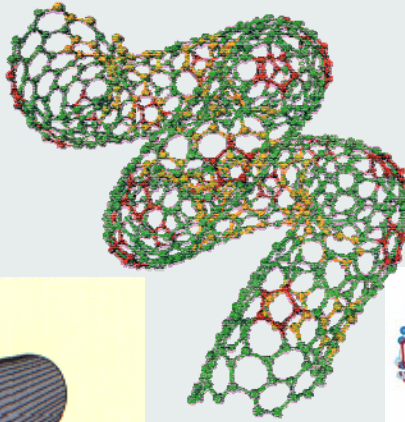
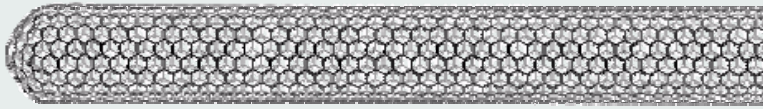
Density:	1.35 g/cm ³
Resistivity	10 ⁻⁴ wcm
Maximum Current Density	10 ⁹ A/cm ²
Thermal Conductivity	~2000 W/mK
Relaxation Time	~10 ⁻¹¹ s
Elastic Behavior	
Young's Modulus (SWNT)	~1 TPa
Young's Modulus (MWNT)	1.28 TPa
Maximum Tensile Strength	~100 GPa

06.11.2006

R. Nesper Oslo Lectures
 Nanochemistry UIO

12

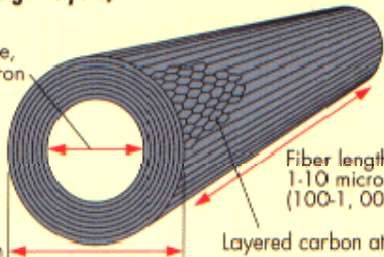
C-Nanotubes - Forms



Rolled-up graphite sheets
(typically eight layers)

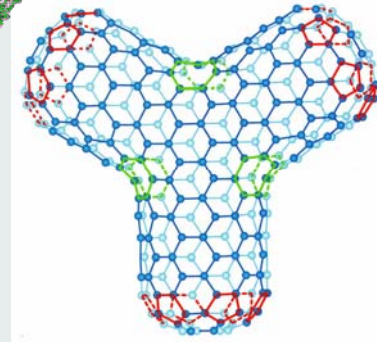
Hollow core,
0.005 micron

0.01
micron



Fiber length,
1-10 microns
(100-1,000:1 l/d)

Layered carbon atoms



06.11.2006

R. Nesper Oslo Lectures
Nanochemistry UIO

13



Multiwalled Carbon Nanotubes

Synthesis below 500 °C

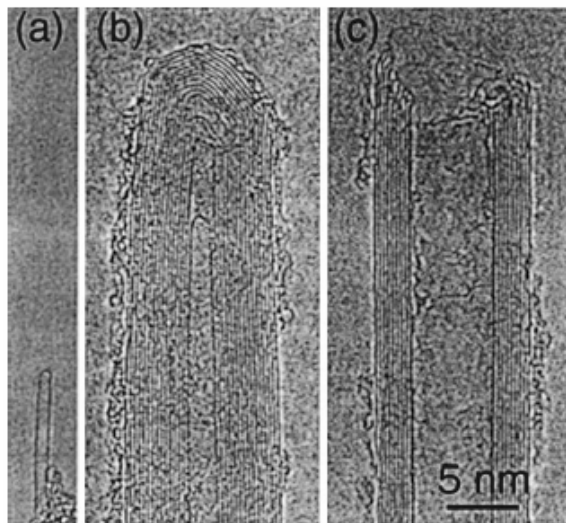
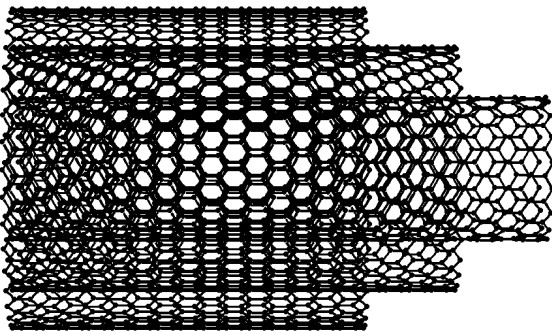
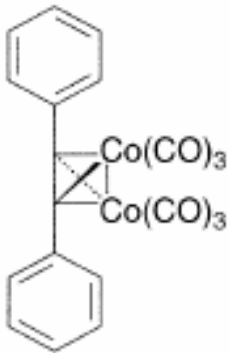


Fig. 2. TEM pictures of the ends of (a) a SWNT, (b) a closed MWNT, and (c) an open MWNT. Each black line corresponds to one graphene sheet viewed edge-on. The micrographs are reproduced at the same magnification.

D ~ 0.34 nm

Nanochemistry UIO



C-Nanotubes - Multiwall Connections

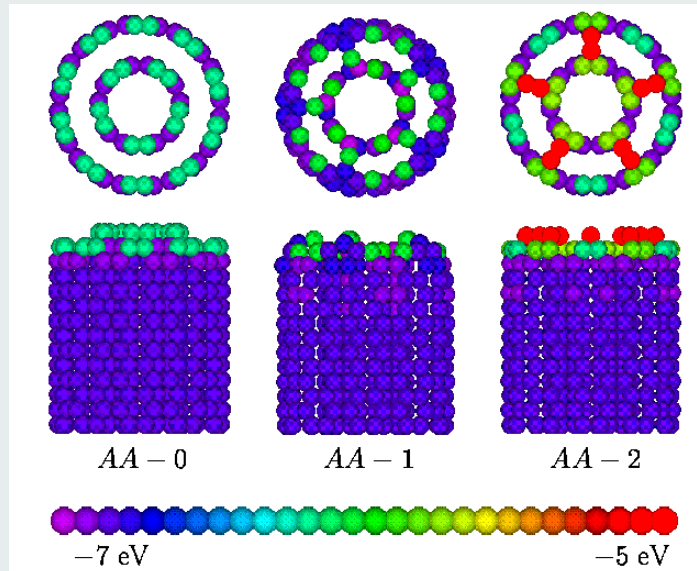
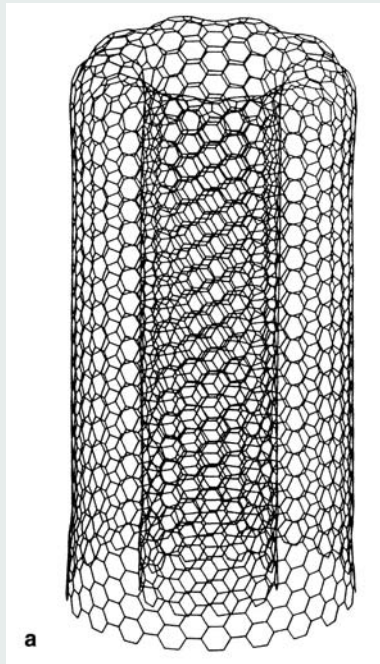


Figure 2

(Young-Kyun Kwon et al., "Morphology and stability of growing multi-wall carbon nanotubes")

Helices, Springs, Actuators

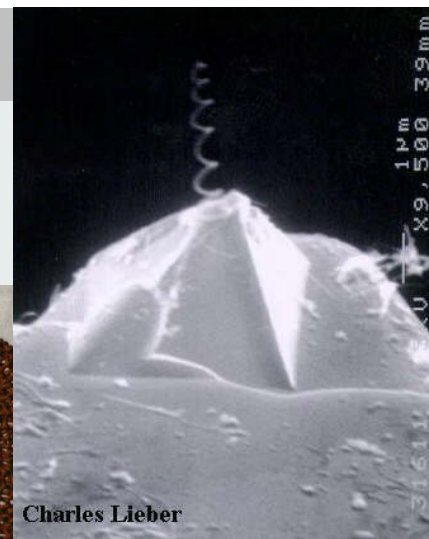


Abb. 6. a) Rasterelektronenmikroskopische (REM)-Aufnahme mehrerer pyrolytisch synthetisierter spiralförmiger Nanoröhrchen. b) Theoretisches Modell der korkenzieherartigen Gebilde.

Other new CNTs ?

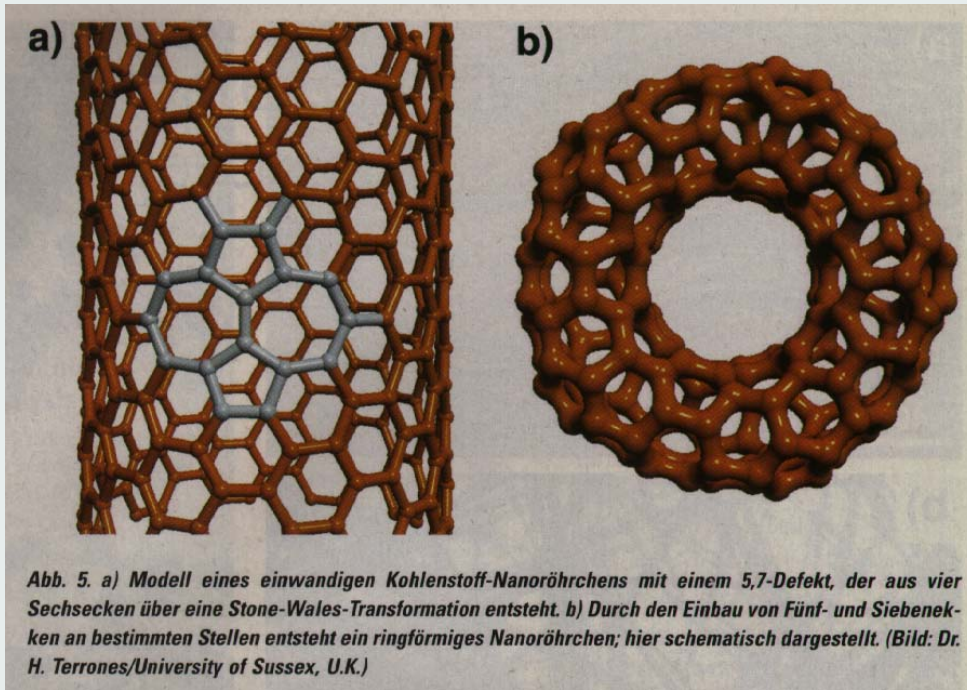


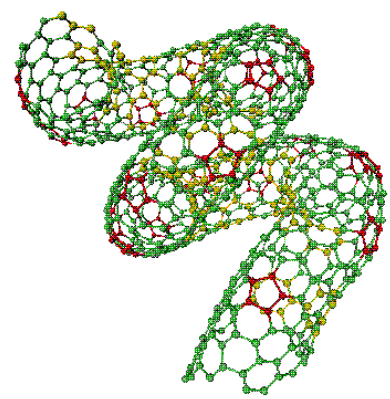
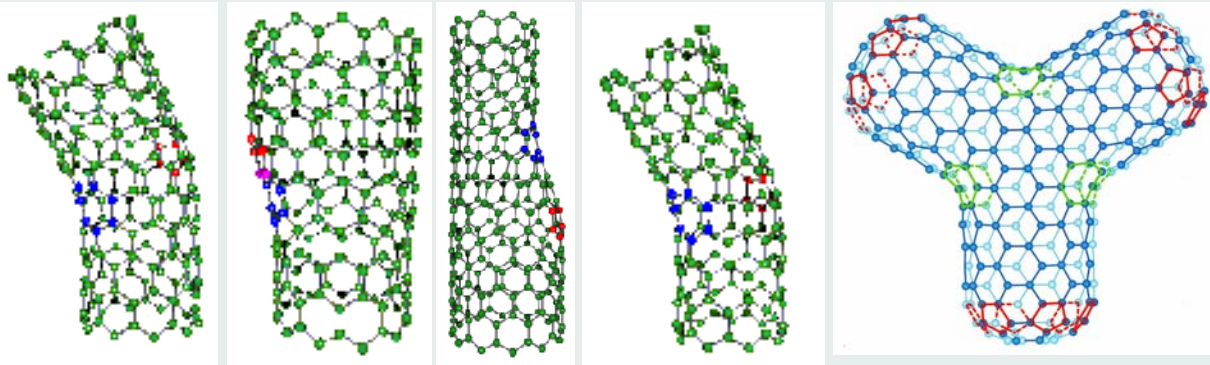
Abb. 5. a) Modell eines einwandigen Kohlenstoff-Nanoröhrchens mit einem 5,7-Defekt, der aus vier Sechsecken über eine Stone-Wales-Transformation entsteht. b) Durch den Einbau von Fünf- und Siebenringen an bestimmten Stellen entsteht ein ringförmiges Nanoröhrchen; hier schematisch dargestellt. (Bild: Dr. H. Terrones/University of Sussex, U.K.)

06.11.2006

R. Nesper Oslo Lectures
Nanochemistry UIO

17

Building Faults, Properties, Electronics

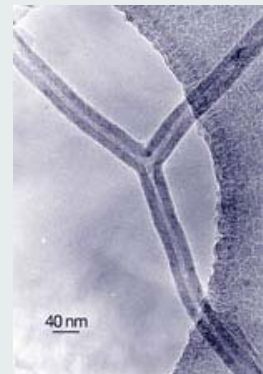


5+7 ring => Diode

But contact resistance !!

Semicond. / metallic CNT
transistor

But no control on helicity!!



06.11.2006

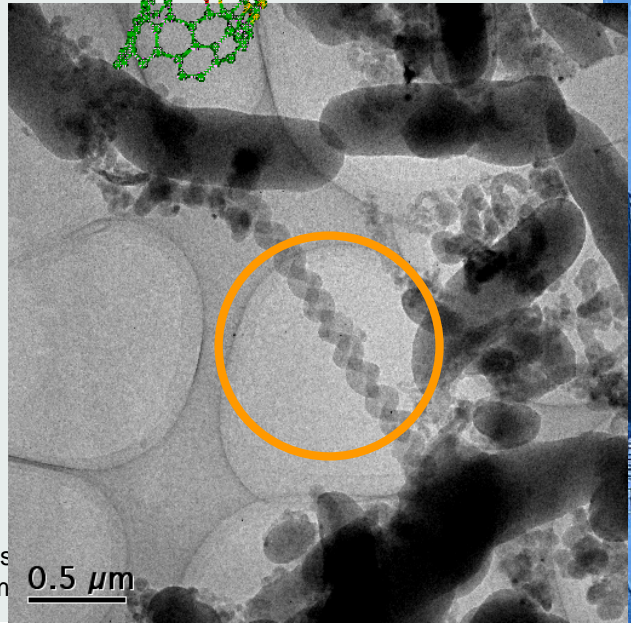
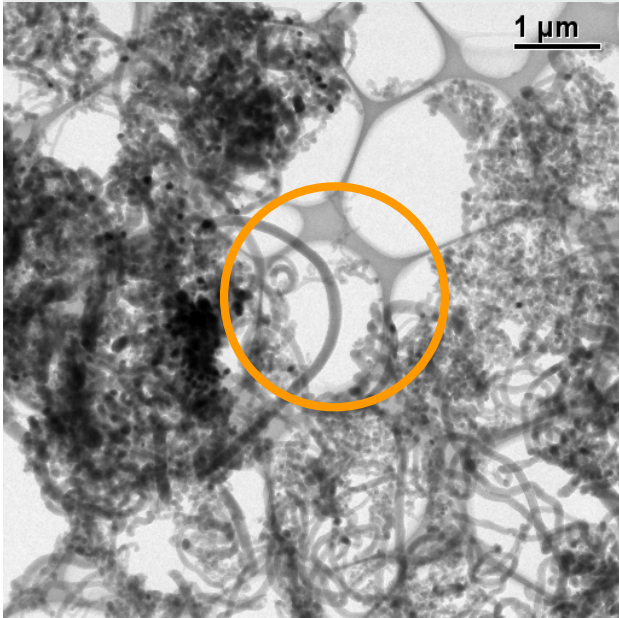
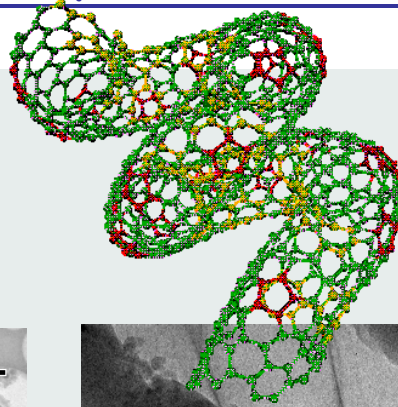
R. Nesper Oslo Lectures
Nanochemistry UIO

18

Low Temperature Syntheses of CNTs and Other C Nanoparticles

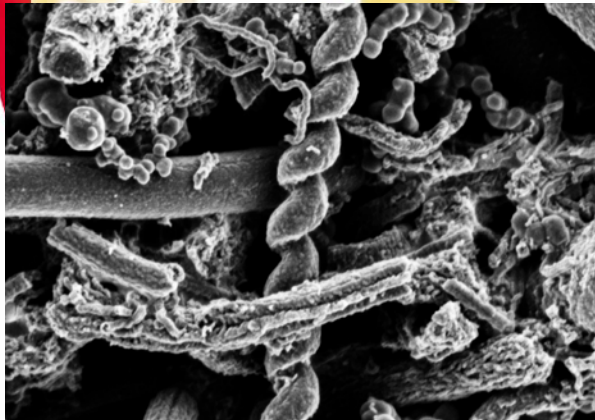
UM HELVETICUM

$T < 500\text{ C}$

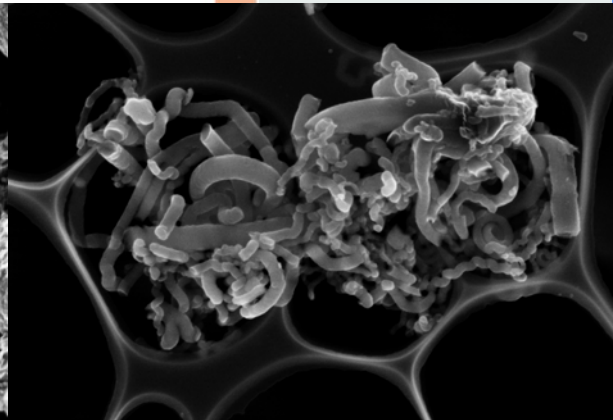


Carbons – All Pasta and Infinite Set ?

R. NESPER ETH ZÜRICH & COLLEGIUM HELVETICUM



EHT = 1.00 kV
 WD = 4 mm
 Signal A = InLens
 File Name = 10-66oben_10.tif
 Date : 30 Jan 2002



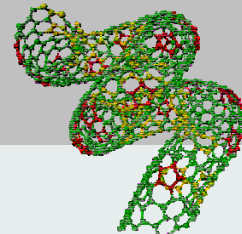
EHT = 5.00 kV
 WD = 3 mm
 Signal A = InLens
 Date : 24 Jul 2001

06.11.2006

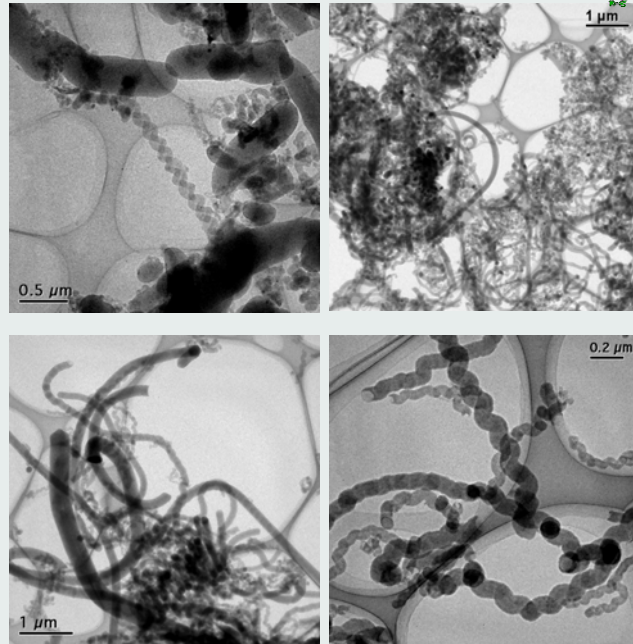
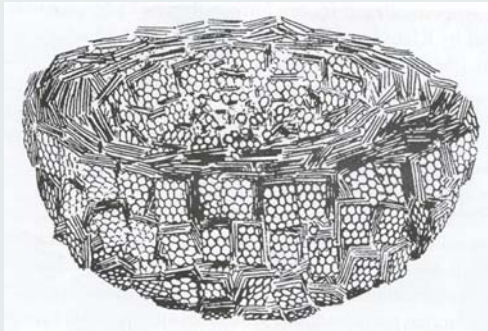
R. Nesper Oslo Lectures
 Nanochemistry UIO

20

Low Temperature Syntheses of CNTs and Other C Nanoparticles



Fish bone structures



06.11.2006

R. Nesper Oslo Lectures
Nanochemistry UIO

21

Low Temperature Syntheses of CNTs

Fish bone structures

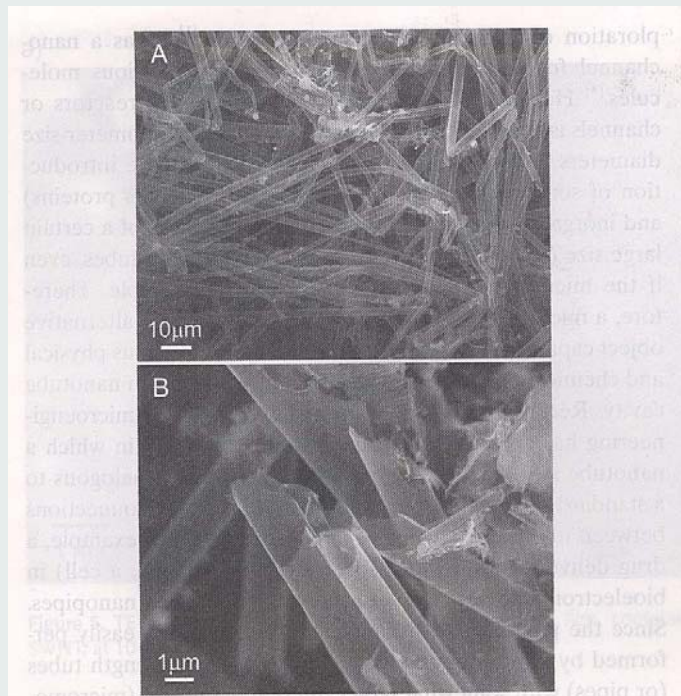
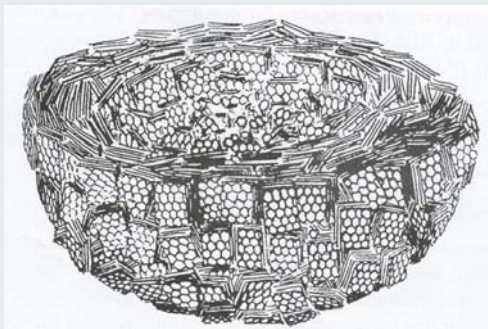
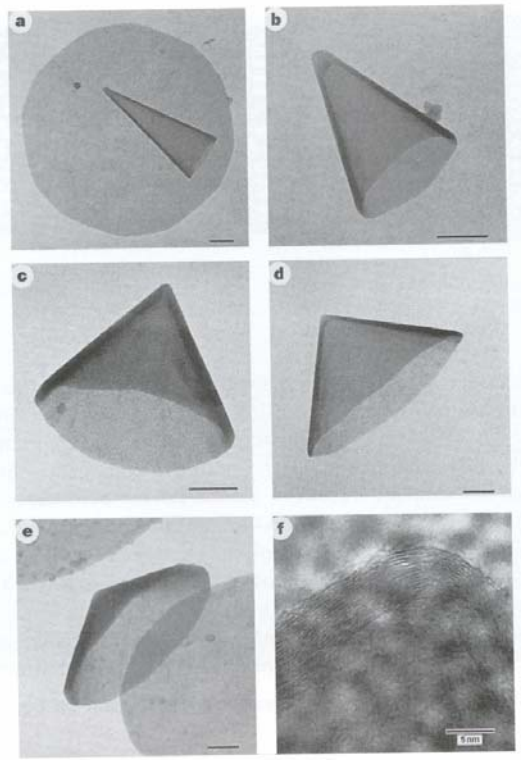


Figure 1. A) Low-magnification SEM image of the carbon microtubes. B) High-magnification SEM image displaying the open ends of the microtubes.

06.11.2006

R. Nesper Oslo Lectures
Nanochemistry UIO

22



06.11.2006

R. Nesper Oslo Lectures
Nanochemistry UIO

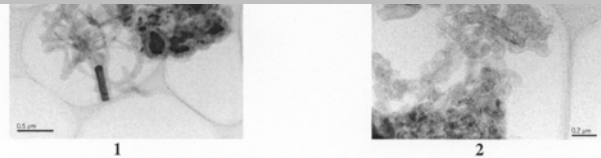


Fig.2 Carbon microstructures obtained (1) after washing with 65% nitric acid (2) after washing with acid and heated to 1000°C in Ar atmosphere

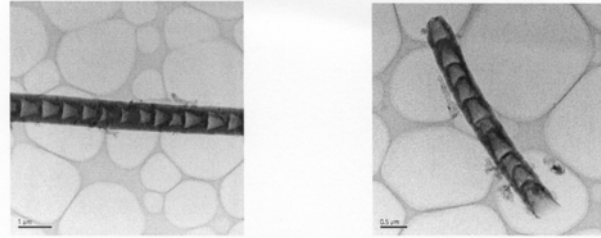


Fig.3 Carbon microstructures obtained (1) after washing with 65% nitric acid (2) after washing with acid and heated to 1000°C in Ar atmosphere

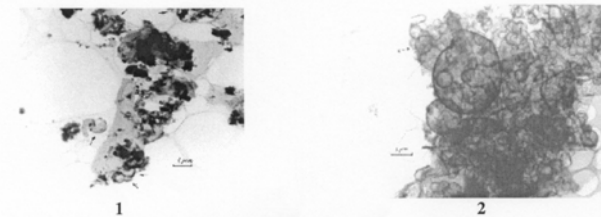


Fig.4 Carbon microstructures obtained (1) after washing with water (2) after washing with concentrated acid

23

Storage in CNTs

In a recent work of Baker and Rogriguez [1] indicate a very large specific hydrogen storage capacity in carbon nanotubes (CNT's) and in herringbone materials. Yet, these results have not been confirmed by any research group in the world [1,2,3,6,7,8], but nevertheless they gave rise to enhanced activity in the field of carbon-based hydrogen storage on the theoretical and on the experimental side.



06.11.2006

R. Nesper Oslo Lectures
Nanochemistry UIO

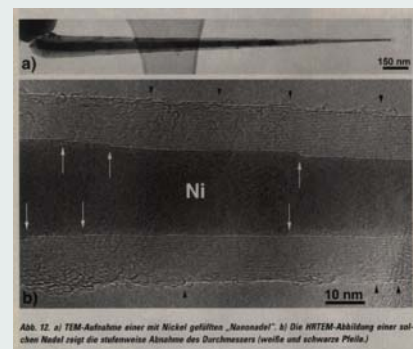
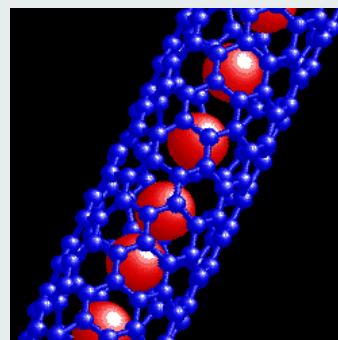


Abb. 12. a) TEM-Aufnahme einer mit Nickel gefüllten „Nanonadel“. b) Die HRTEM-Abbildung einer solchen Nadel zeigt die stufenweise Abnahme des Durchmessers (weiße und schwarze Pfeile.)



24

H₂ - Storage in C-NTs ?

wrong !! →

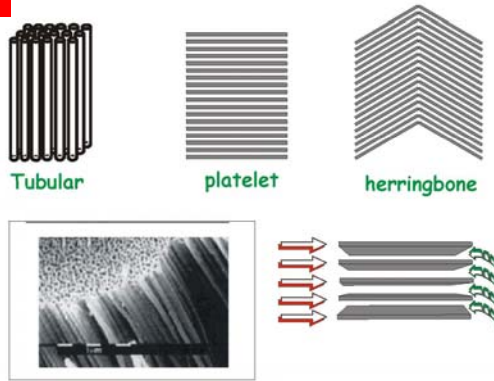
Baker, N. Rodriguez et al., J.Phys.Chem. B 102, 423 (1998)

Baker & Rodriguez

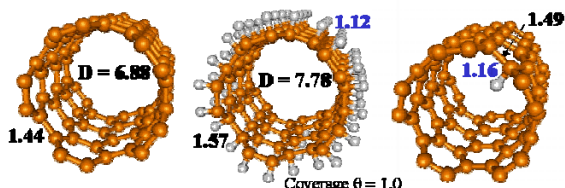
65wt% !!???

M. Parrinello

max. 14wt%



Hydrogen adsorption on (5,5) SWNT



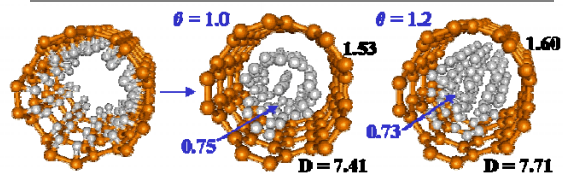
< Binding energy (eV/bond) >

	C-C	C-H	C-H
DFTB	-9.14	-2.65	-0.83
LDA	-8.41	-2.10	-1.50
GGA	-7.48	-1.75	-1.28

06.11.2006

Nanotubes Research Lab

Hydrogen storage in (5,5) SWNT



	DFTB (LDA:GGA)	DFTB
• Binding energy (eV/H ₂)	-4.57 (-3.16:-2.24)	-4.01
• Wall-H ₂ repulsive energy (eV/H ₂)	0.70 (0.47:0.74)	0.78
• H ₂ -H ₂ repulsive energy (eV/H ₂)	0.89 (0.81:1.19)	1.11

- H₂ molecules exist inside nanotubes.
- H₂ can be stored inside nanotubes with coverage > 1.0.

Nanotubes Research Lab

Catalyst Patterning for Growth of CNTs

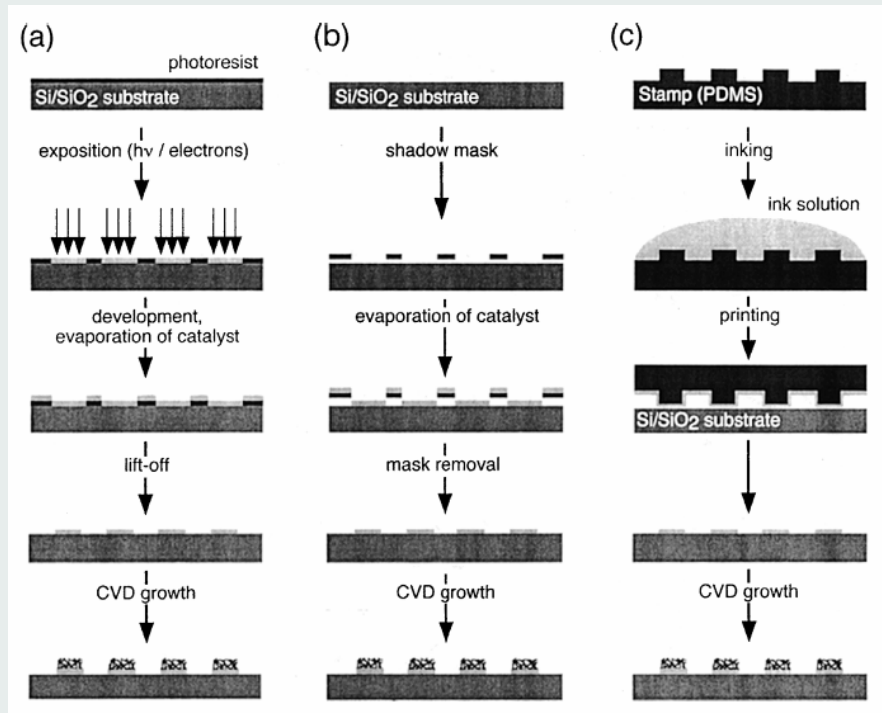


Fig. 4. Techniques to produce patterns of catalysts for the selective growth of carbon nanotubes: (a) standard lithography, (b) shadow-masking, (c) soft lithography.

06.11.2006

26

Hierarchical Order – Aggregations

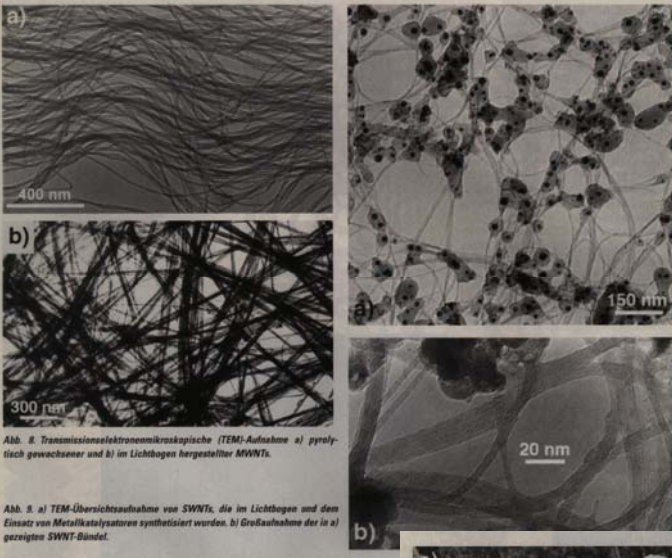
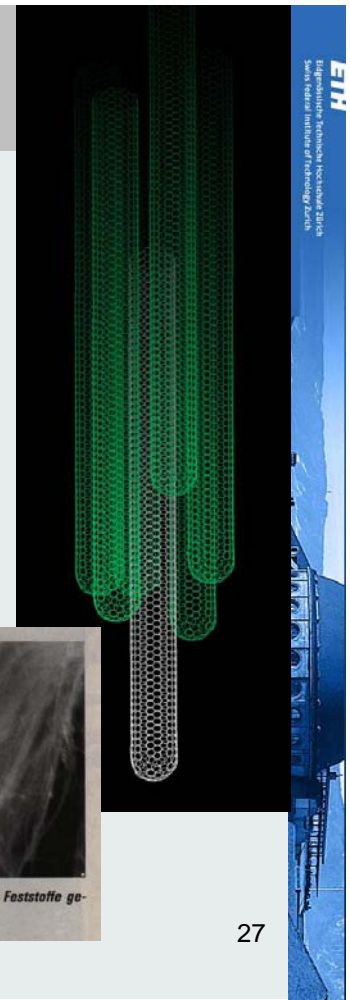


Abb. 8. Transmissionselektronenmikroskopische (TEM)-Aufnahme a) pyrolytisch gewachsener und b) im Lichtbogen hergestellter MWNTs.

Abb. 9. a) TEM-Übersichtsaufnahme von SWNTs, die im Lichtbogen und dem Einsatz von Metalkatalysatoren synthetisiert wurden. b) Großaufnahme der in a) gezeigten SWNT-Bündel.



06.11.2006

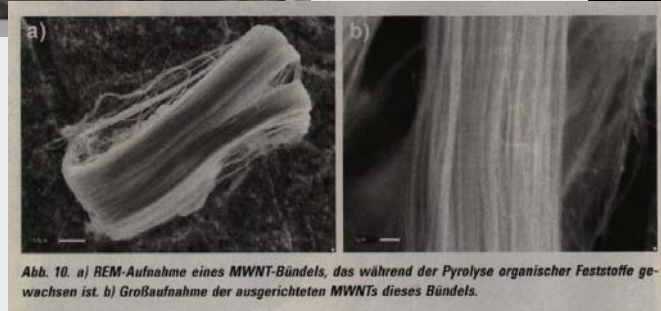
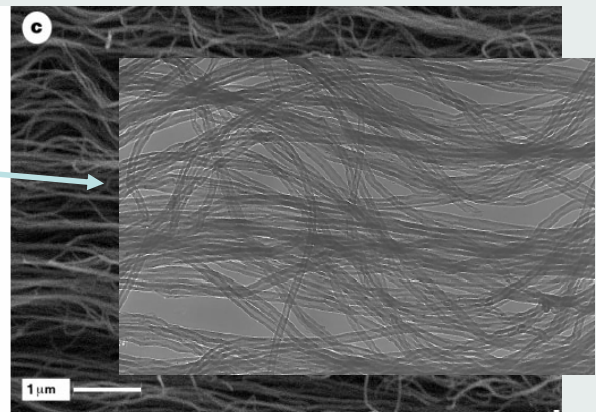
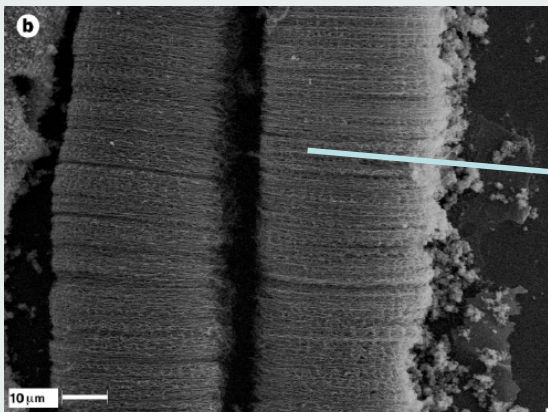
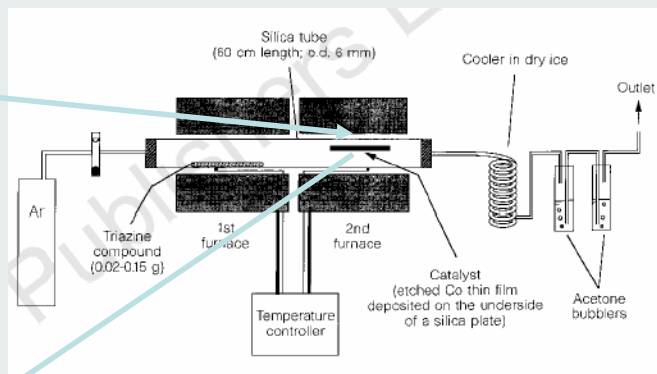
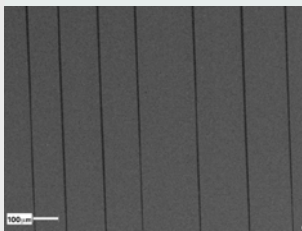


Abb. 10. a) REM-Aufnahme eines MWNT-Bündels, das während der Pyrolyse organischer Feststoffe gewachsen ist. b) Großaufnahme der ausgerichteten MWNTs dieses Bündels.

Nanochemistry UIO

27

Hierarchical Order – Carpets Predefined



06.11.2006

R. Nesper Oslo Lectures
Nanochemistry UIO

28

Hierarchical Order – Carpets etc.

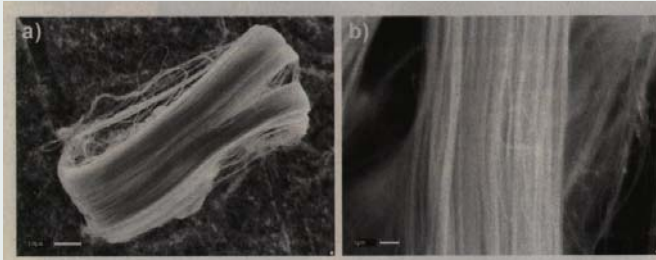
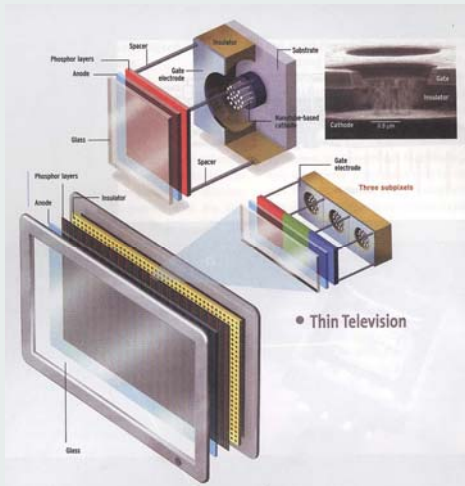
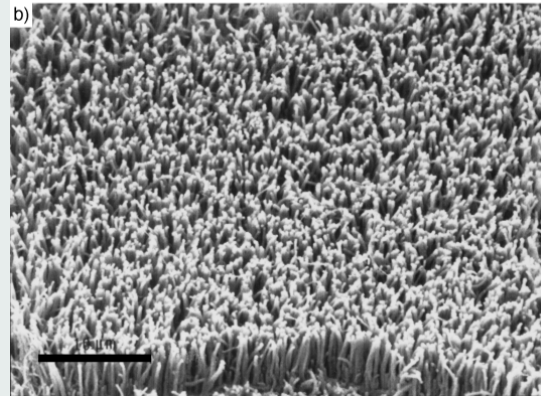
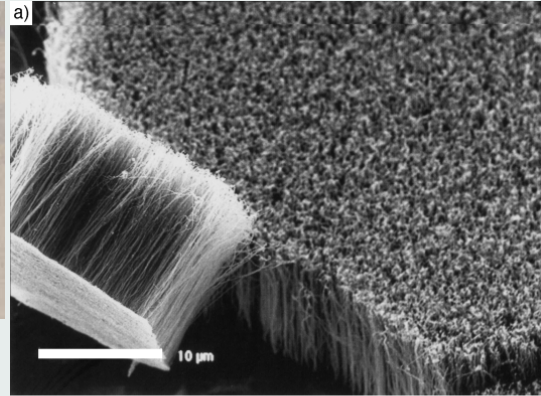


Abb. 10. a) REM-Aufnahme eines MWNT-Bündels, das während der Pyrolyse organischer Feststoffe gewachsen ist. b) Großaufnahme der ausgerichteten MWNTs dieses Bündels.



06.1

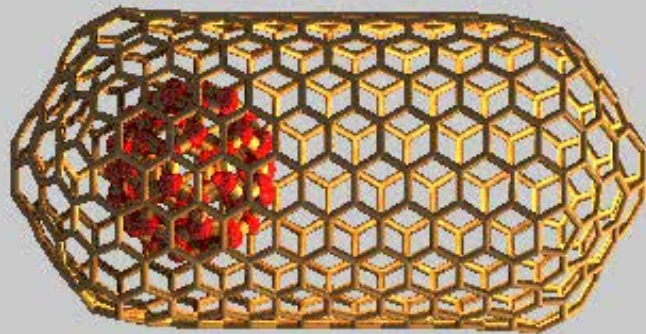
Nesper Oslo Lectures
Nanochemistry UIO

29



Carbon Nanotubes Models

<http://www.pa.msu.edu/cmp/csc/nanotube.html>



06.11.2006

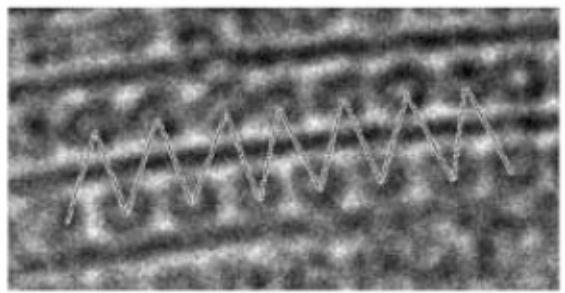
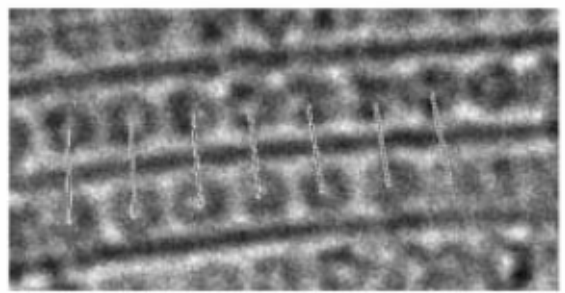
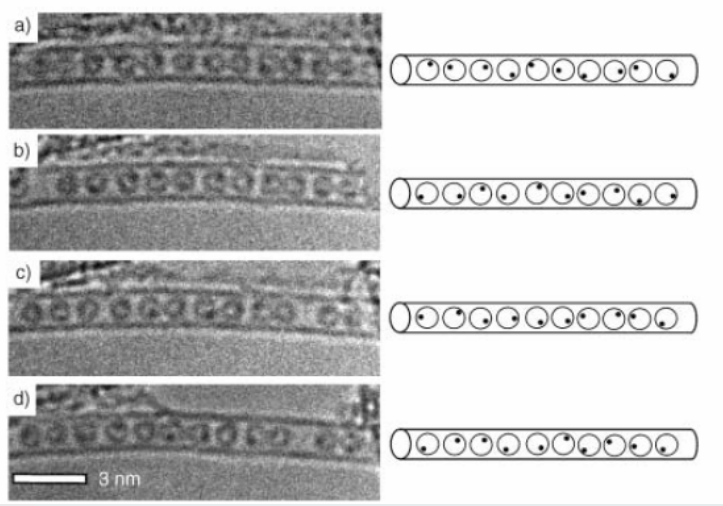
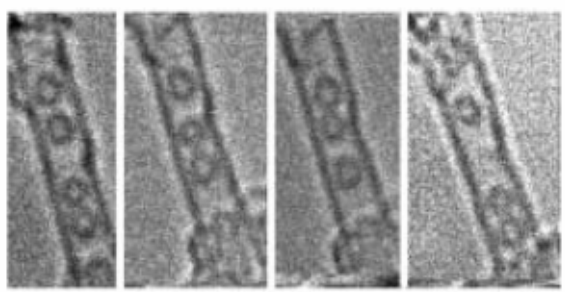
R. Nesper Oslo Lectures
Nanochemistry UIO

30



Filling of Carbon Nanotubes

HELVETICUM



06.11.2006

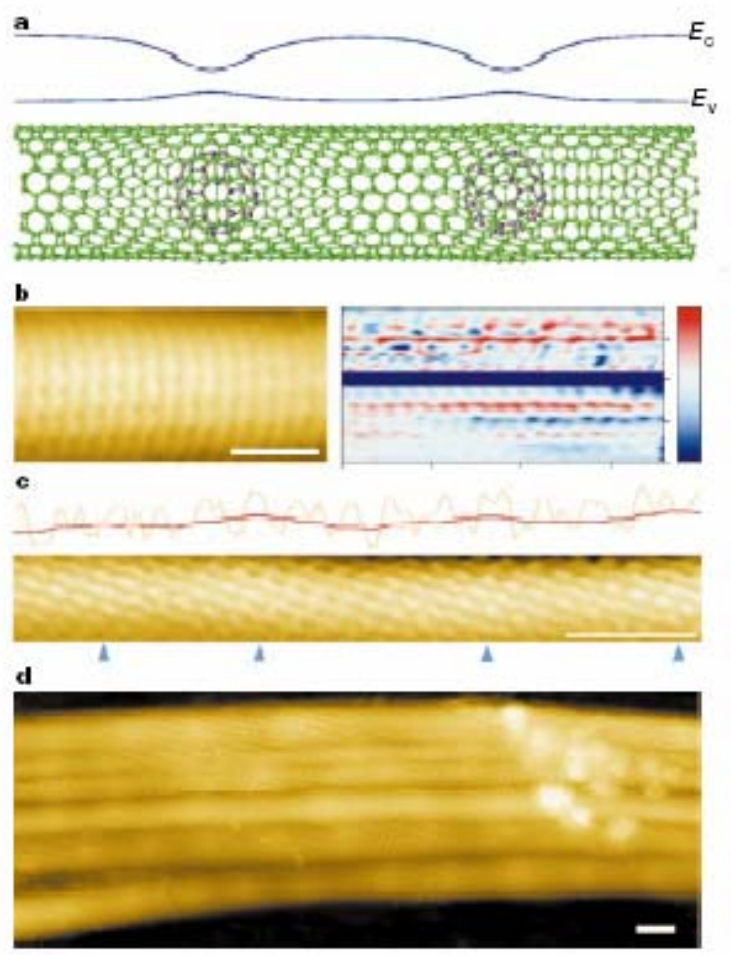
R. Nesper Oslo Lectures
Nanochemistry UIO

31

Valence & conduction bands

R. NESPER ETH ZÜRICH & COLLEGIUM HELVETICUM

- Elastic strain
- STM topography
- Atomic resolution
- SWT bundle



06.11.2006

R. N
N

Applications of CNTs - Thermocouple

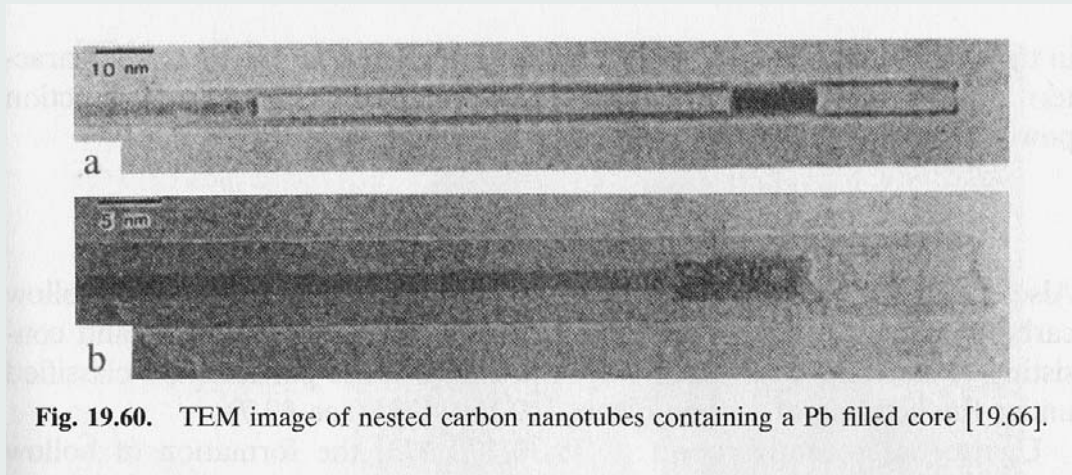
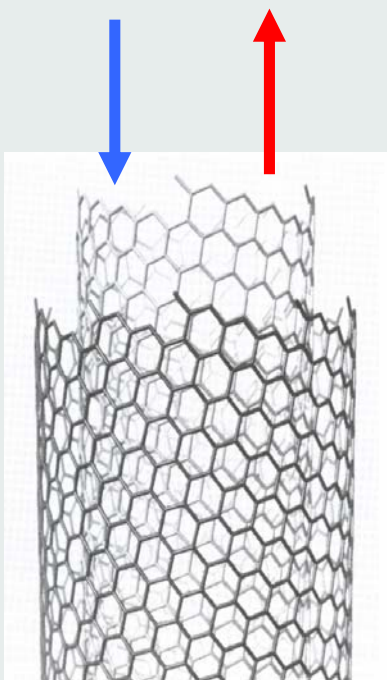


Fig. 19.60. TEM image of nested carbon nanotubes containing a Pb filled core [19.66].

Tube-in-Tube

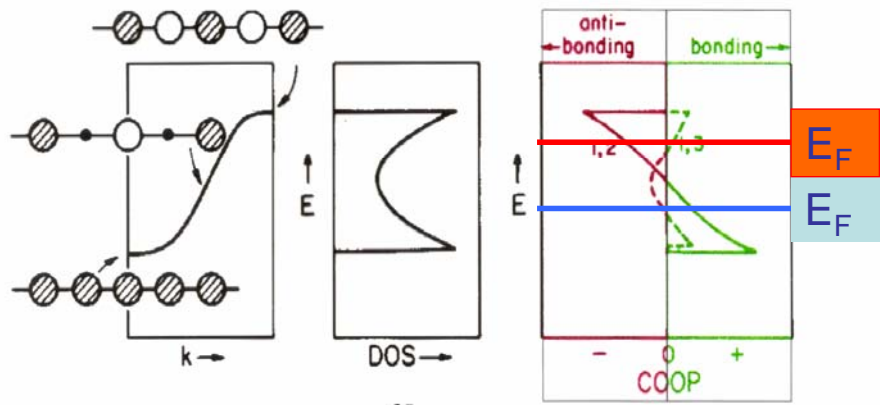
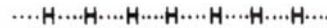
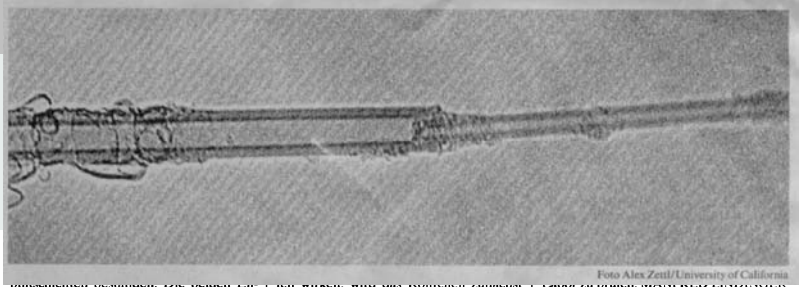


Flinkes Nanoröhrchen schwingt wie winziges Federpendel

Nanoröhrchen aus Kohlenstoff gewinnen wegen ihrer ungewöhnlichen Eigenschaften für die Wissenschaft zunehmend an Bedeutung. Einerseits sind die zylindri-

den der Röhrchen waren zunächst durch mehrlagige Kappen abgeschlossen. Zettl und seine Kollegen entfernten die Kappe an einem Ende und ergriffen die inner-

wieder in das Innere der Graphithülle zurückgezogen. Dort besitzt es aber genügend kinetische Energie, am anderen Ende wieder herauszuschieben. Hat sich



Field Emission Displays

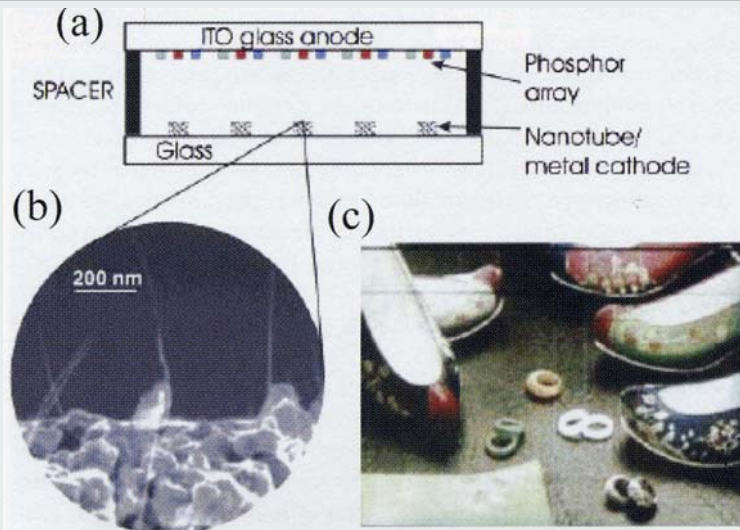
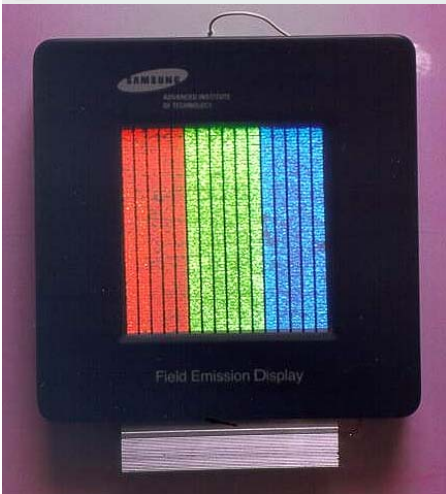


Fig. 8.14. (a) Schematic illustration of a flat panel display based on carbon nanotubes. ITO, indium tin oxide. (b) SEM image of an electron emitter for a display, showing well-separated SWNT bundles protruding from the supporting metal base. (c) Photograph of a 5 in (13 cm) nanotube field emission display made by Samsung. Reproduced from ref. [187], with permission.

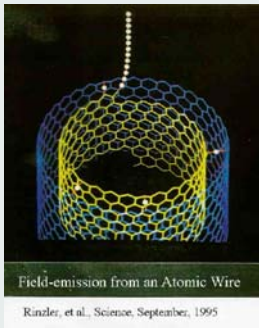
06.11.2006

R. Nesper Oslo Lectures
 Nanochemistry UIO

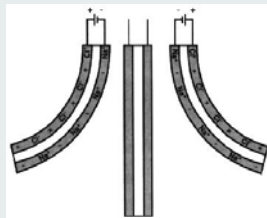
35

(C)NT-Applications

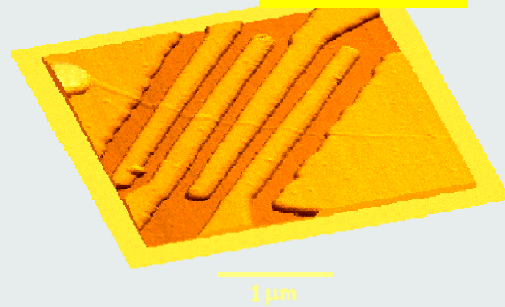
emission tip



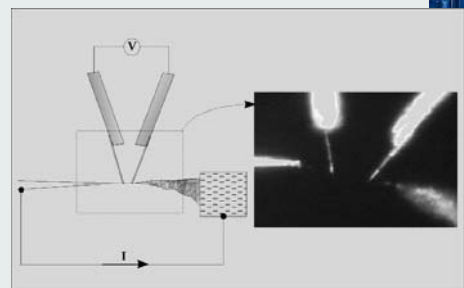
ion sensor
 actuator



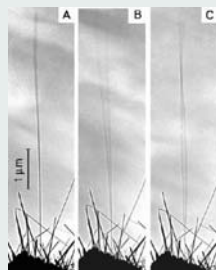
Conductor
 rectifier
 transistor
 sensor



nano tips



??



06.11.2006

R. Nesper Oslo Lectures
 Nanochemistry UIO

C-NT Sensor

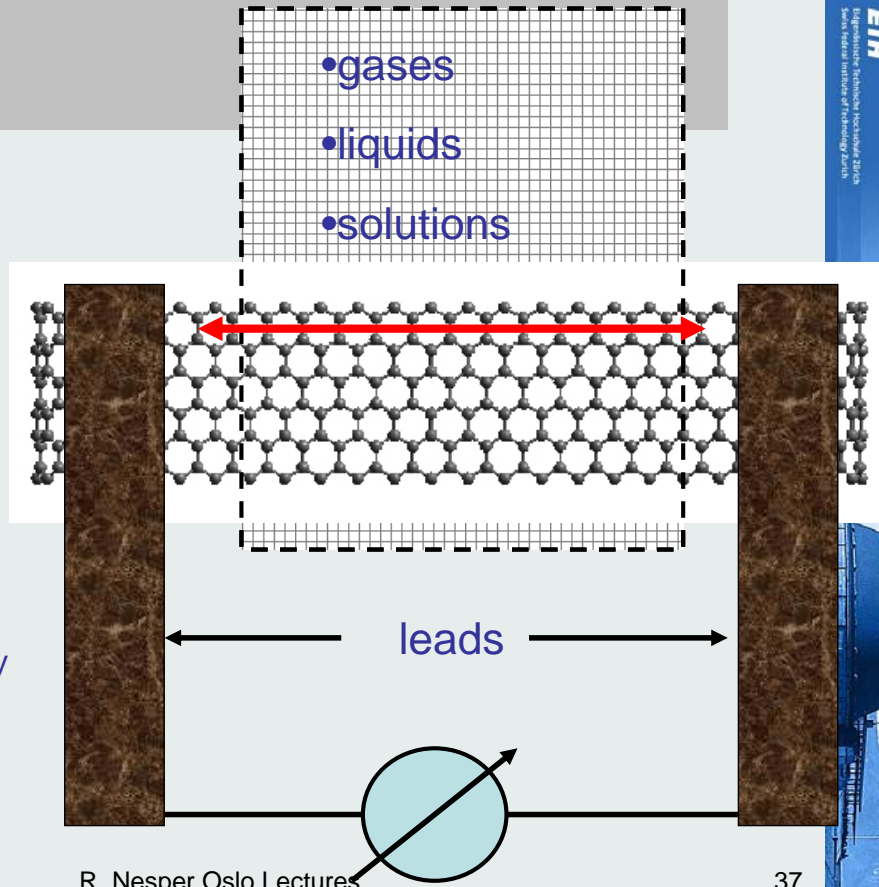
R. NESPER ETH ZÜRICH & COLLEGIUM HELVETICUM

Surface electron
conductance

Adsorbed species

strongly change conductivity

- gases
- liquids
- solutions



06.11.2006

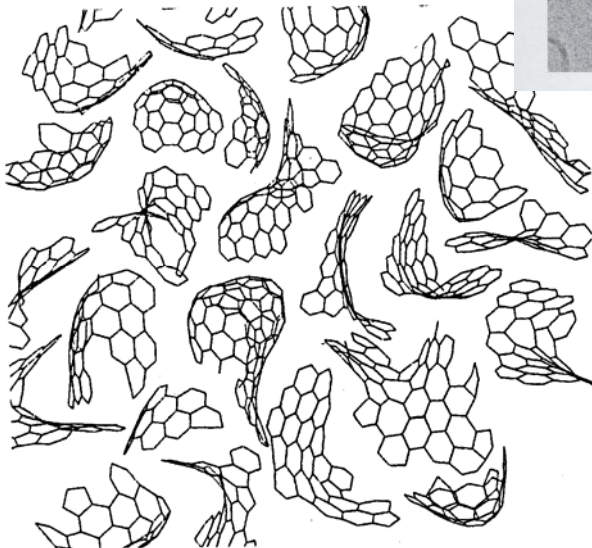
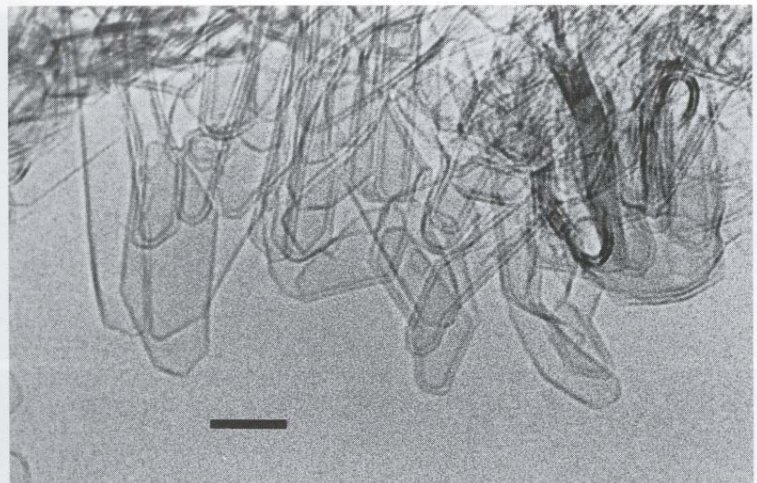
R. Nesper Oslo Lectures
Nanochemistry UIO

37



New Carbons ?

GIUM HELVETICUM



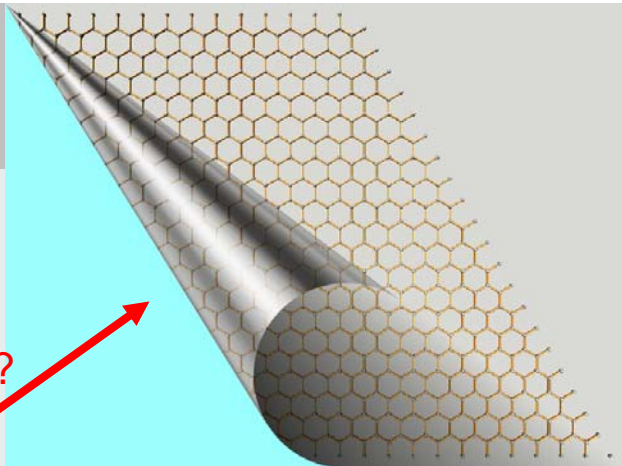
Oslo Lectures
emistry UIO

38

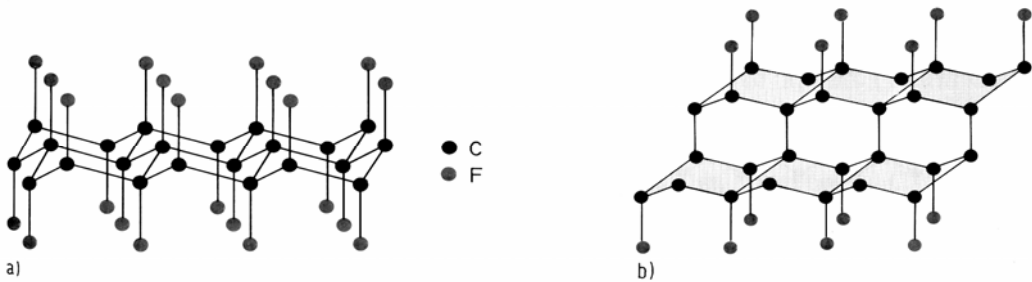
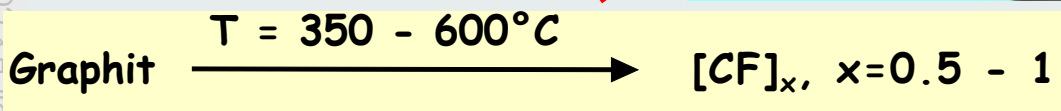


Derivates of Graphite

D. NEEDEE, ETH ZÜRICH & COLLEGIUM HELVETICUM



???



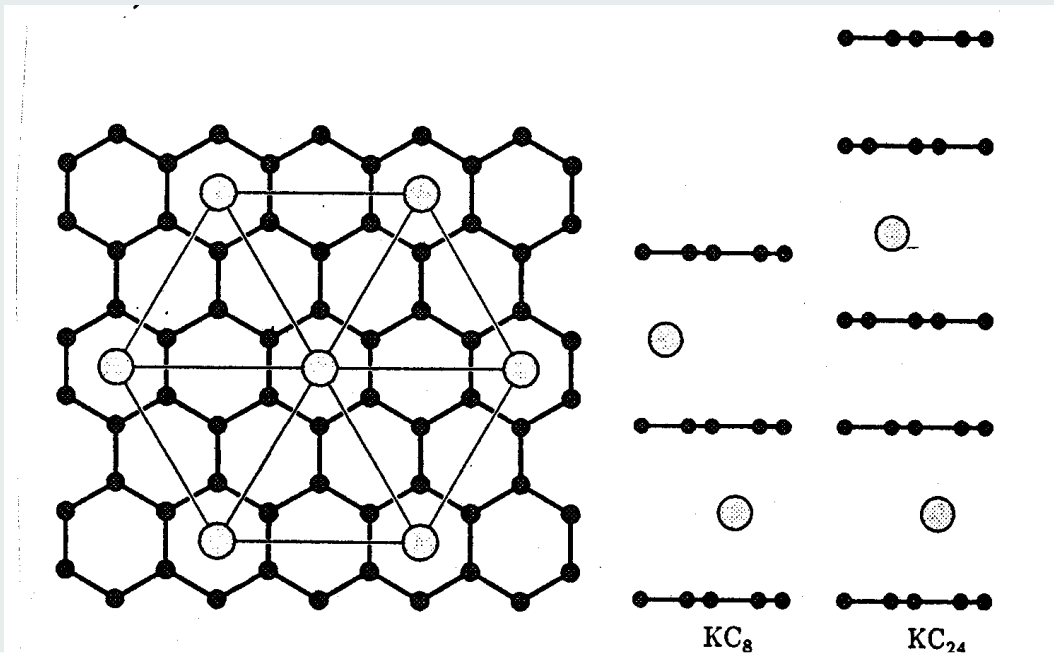
06.11.2006

R. Nesper Oslo Lectures
Nanochemistry UIO

39

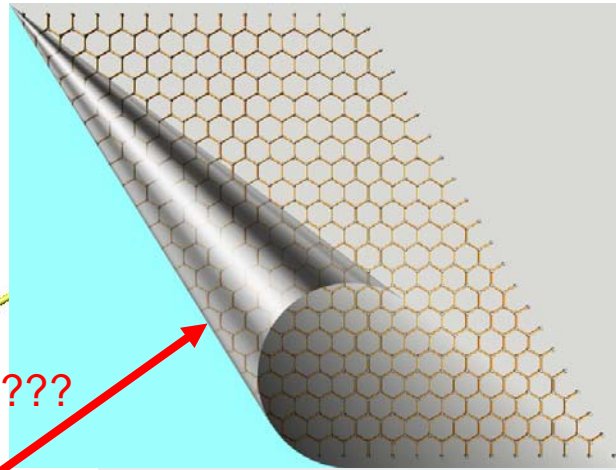
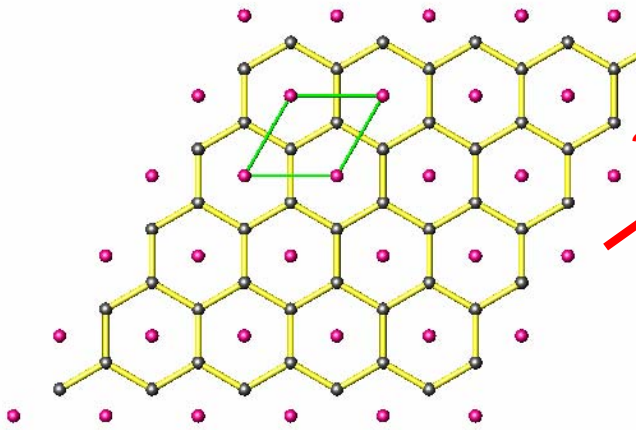
Exfoliate Graphite Intercalation Compounds?

R. NESPER, ETH ZÜRICH & COLLEGIUM HELVETICUM



40

Heterographites



MgB₂
 AlB₂
 MgB₂C₂
 LiBC

06.11.2006

R. Nesper Oslo Lectures
 Nanochemistry UIO

41



Graphite-related Superconductors

The superconducting materials demonstrate a **zero electrical resistivity** in a certain range of temperature, current and magnetic field.

Their maximum values are called:

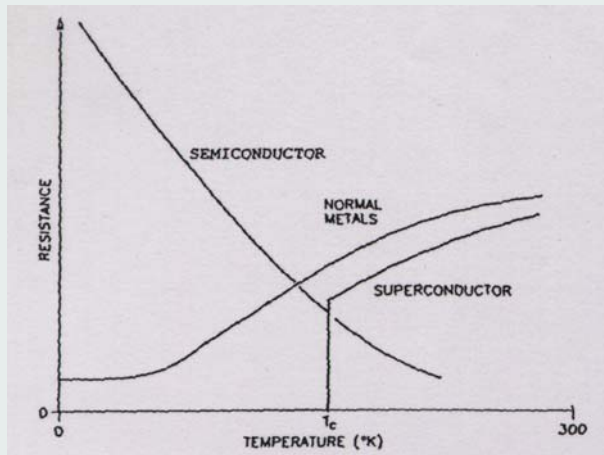
critical temperature (T_c)

critical current density (J_c)

critical magnetic field (H_c)

MgB₂
~~MgB₂C₂~~
~~LiBC~~
~~AlB₂~~

Ca_x-graphite
 Yb_x-graphite
~~„Li_{0.5}BC“ T_c = 90K~~



R. NESPER ETH ZÜRICH & COLLEGIUM HELVETICUM



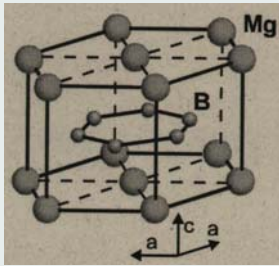
06.11.2006

R. Nesper Oslo Lectures
 Nanochemistry UIO

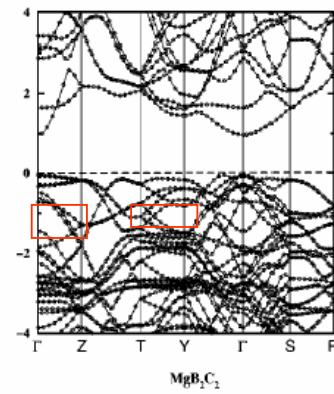
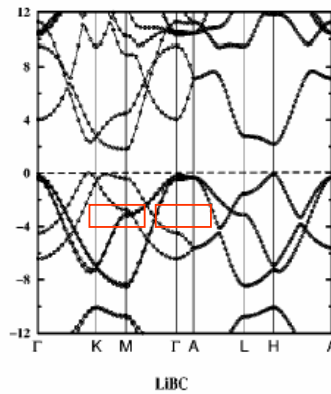
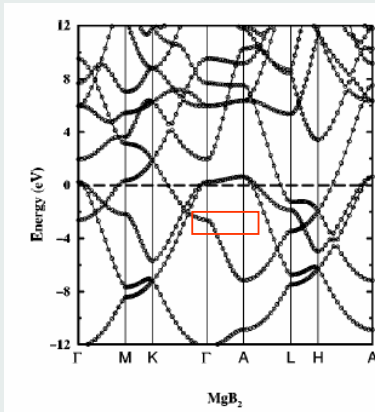
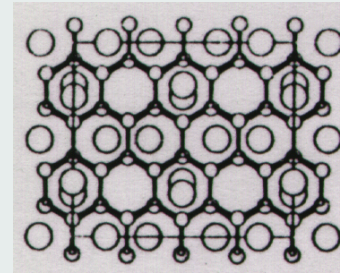
42

Supraleitung in MgB_2 , $LiBC$ and MgB_2C_2

R. NESPER ETH ZÜRICH & COLLEGIUM HELVETICUM



MgB_2
 MgB_2C_2
 $LiBC$
 $Li_{0.5}BC$ $T_c=90K$



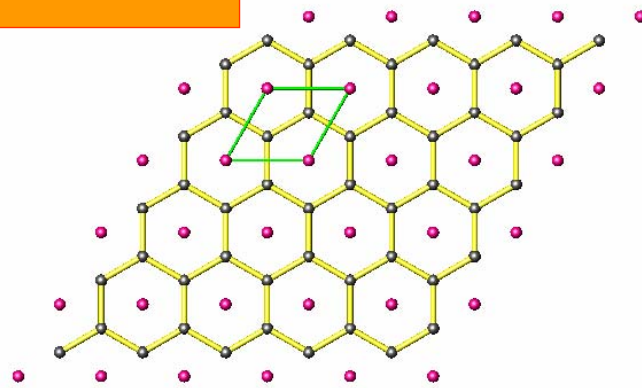
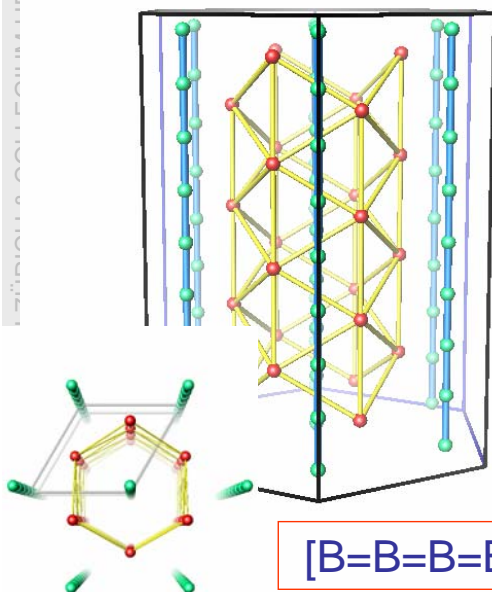
06.11.2006

R. Nesper Oslo Lectures
 Nanochemistry UIO

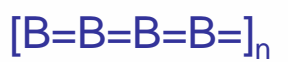
43



MgB_2 and its Analoga Wire Preparation ?



J.M. Reinoso, F. Ottinger, M. Wörle, R. Nesper,
 Method for producing a super-conducting
 material made of MgB_2 , Patent No
 WO0207149909/2002

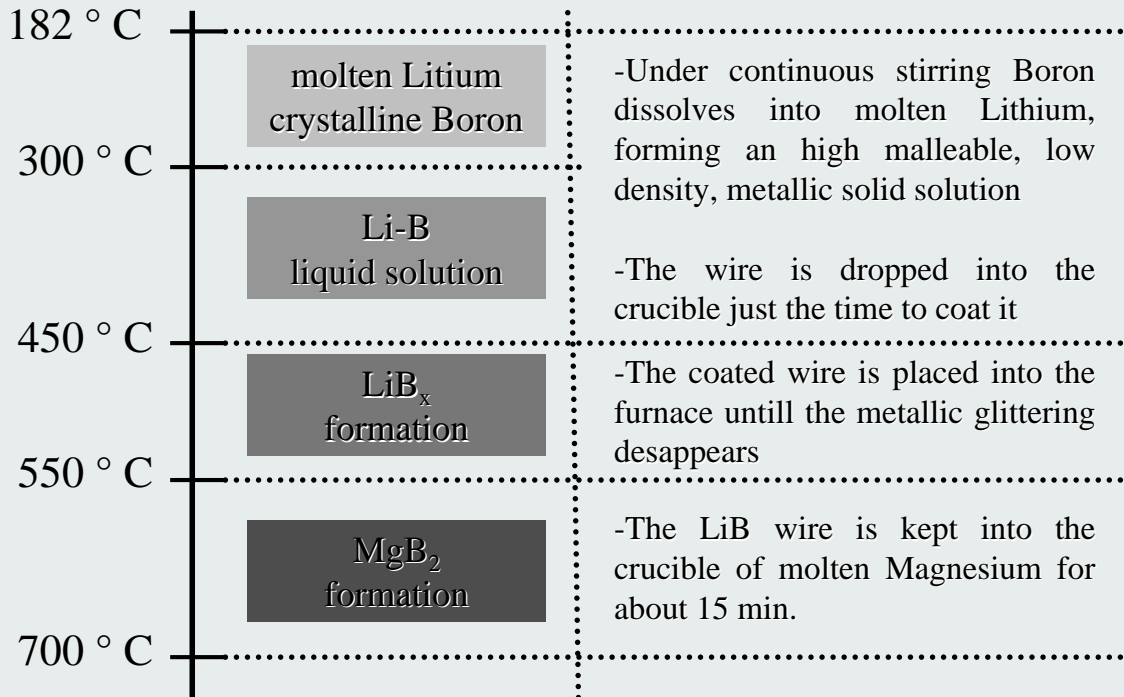


R. Nesper Oslo Lectures
 Nanochemistry UIO

44



Morphologie Preserving Transformation



- Sublimation of Mg / Mg_xLi_y under High vacuum, 630 ° C, 8 h

Preparing Wires and Rods

Li-B mixture



- The inner part does not react completely

LiB_x compound



- The resulting coating is highly porous

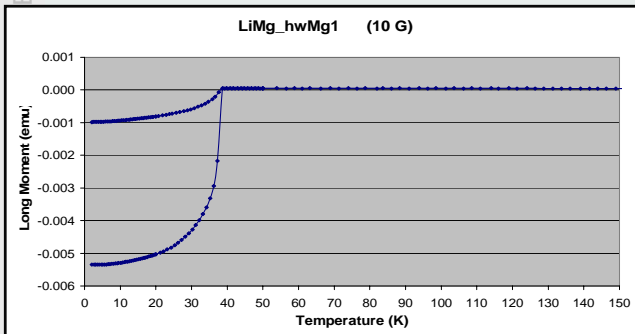
MgB₂



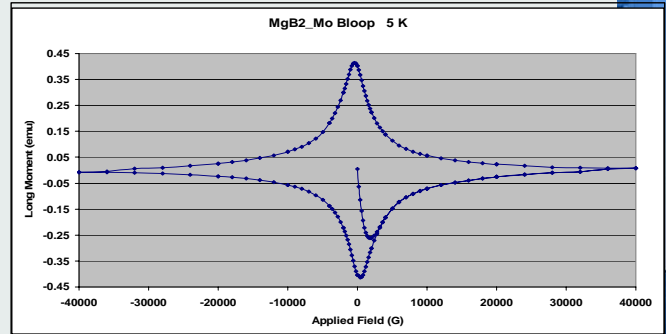
- Formation of oxidic layer can occur between the wire and the coating

Magnetische Messungen

reines MgB_2 $\chi(T)$



MgB_2 $\chi(H)$



06.11.2006

R. Nesper Oslo Lectures
Nanochemistry UIO

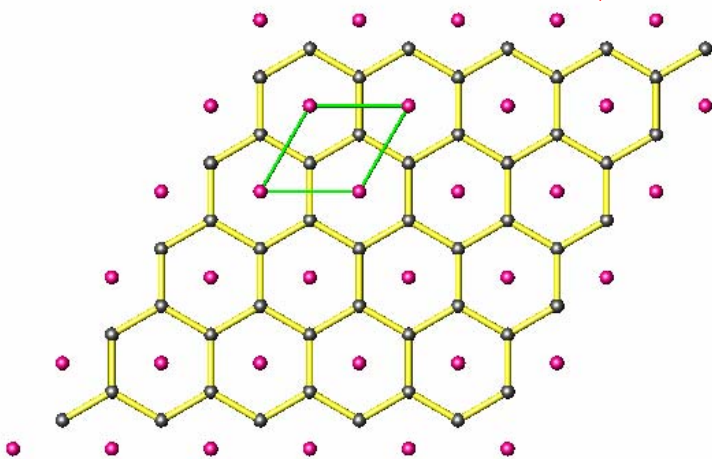
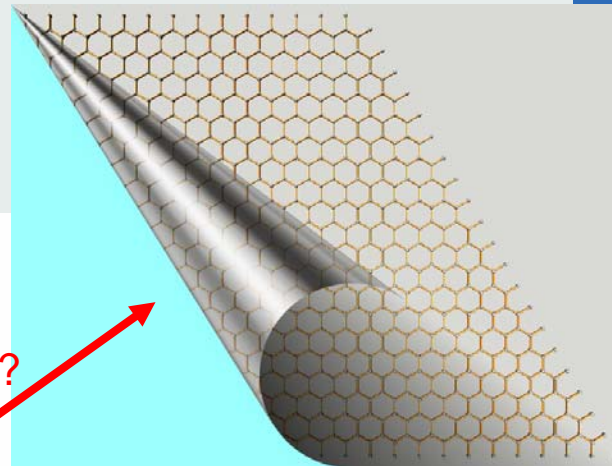
47

Heterographites –

MgB_2
 MgB_2C_2
 LiBC

„ $\text{Li}_{0.5}\text{BC}$ “ $T_c=90\text{K}$

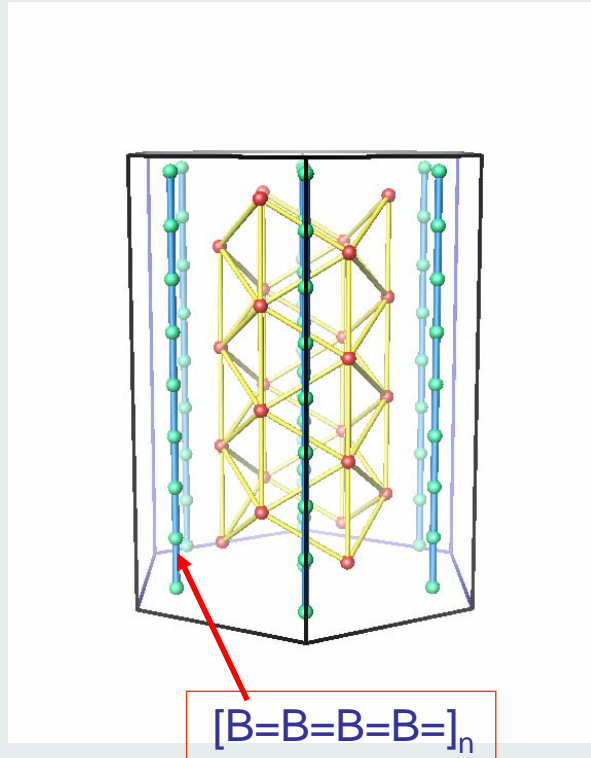
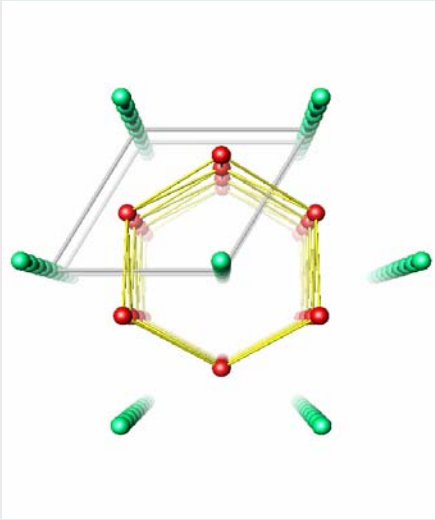
???



Scrolled Ionic Compounds ?

48

Chaoite – Substitute ?



06.11.2006

R. Nesper Oslo Lectures
Nanochemistry UIO

49